FLOOD MODELING AND THE INFLUENCE OF DIGITAL TERRAIN MODELS:
A CASE STUDY OF THE SWANNANOA RIVER IN NORTH CAROLINA

A Thesis
by
MONICA JEAN DAVIS

Submitted to the Graduate School
Appalachian State University
in partial fulfillment of the requirements for the degree of
MASTER OF ARTS

May 2015
Major Department: Geography and Planning

FLOOD MODELING AND THE INFLUENCE OF DIGITAL TERRAIN MODELS:
A CASE STUDY OF THE SWANNANOA RIVER IN NORTH CAROLINA

A Thesis
by
MONICA JEAN DAVIS
May 2015

APPROVED BY:

_____
Jeffrey D. Colby, *Ph.D.*
Chairperson, Thesis Committee

_____
John C. Pine, *Ph.D.*
Member, Thesis Committee

_____
J. Greg Dobson
Member, Thesis Committee

_____
Kathleen Schroeder, *Ph.D.*
Chairperson, Department of Geography and Planning

_____
Max C. Poole, *Ph.D.*
Dean, Cratis D. Williams School of Graduate Studies

Abstract

FLOOD MODELING AND THE INFLUENCE OF DIGITAL TERRAIN MODELS:
A CASE STUDY OF THE SWANNANOA RIVER IN NORTH CAROLINA

Monica Jean Davis
B.S. & B.F., Purdue University
M.A., Appalachian State University

Chairperson: Jeffrey D. Colby

An increase in flood disasters nationally and internationally has underscored the need for accurate flood modeling regarding flood insurance and emergency response. According to the National Research Council, topographic data is the most important variable in determining flood modeling accuracy. Increasing availability of airborne light detection and ranging (LiDAR) data warrants the investigation of the optimal resolution or range of resolutions needed to represent digital terrain models (DTMs) for accurate operational flood modeling.

Few studies have focused on flood modeling in mountain environments. Within the Appalachian Mountains of western North Carolina, the Swannanoa River was selected for this study based on unique physical characteristics, a substantial built environment within the 100 year (100yr) floodplain, and significant recorded levels of historical flooding.

Flood modeling accuracy was evaluated for the Swannanoa River using elevation data from two different sources. LiDAR elevation data were represented at a range of equivalent resolutions 3.77m, 6m, 8m, 10m, 12m, 15m, 20m, 25m, and 30m, and United Stated Geological Survey (USGS) Level 2 digital elevation model (DEM) data were represented at 10m and 30m resolutions. Each elevation was combined with a series of flood recurrence intervals 10yr, 25yr, 50yr, 100yr, and 500yr for testing. A variety of descriptive and inferential statistics were used to evaluate water surface profiles and depth grids generated using the United States Army Corp of Engineer's (USACEs) Hydrologic Engineering Centers – River Analysis System (HEC-RAS) hydraulic model and Environmental Systems Research Institute's (ESRIs) ArcGIS software.

Acknowledgements

I would like to thank my thesis chairperson, Dr. Jeffrey D. Colby, and my committee Dr. John Pine and Greg Dobson for their support, direction, and patience throughout the thesis process. I would also like to thank Brown and Caldwell for the use of their HEC-RAS hydraulic model and access to their Structure Inventory Database. Lastly, I would like to thank the National Environmental Modeling and Analysis Center in Asheville, NC for data used in this research effort.

Dedication

I dedicate this thesis to my parents Michael J. and Joyce A. Davis for their continuous

encouragement, advice, and support.

Table of Contents

List of Tables

List of Figures

Chapter 1

INTRODUCTION

Floods are responsible for two thirds of all Federal Emergency Management Agency (FEMA) federally designated disasters under the Stafford Act within the United States (U.S.) (National Research Council (NRC), 2009). Internationally, the European Union Flood Directive requires member states to coordinate flood reduction efforts and assess the risk of flooding (European Commission, 2007). The U.S. National Research Council (NRC), a section on the U.S. National Academies, created a Committee on FEMA Flood Maps (NRC, 2009). This committee studied the effects of hydrologic, hydraulic, and elevation data on flood map accuracy. Elevation data accuracy was found to be the most important factor in determining flood extent, water surface elevation, and base flood elevation (BFE) for flood risk mapping (Dewberry, 2011; NRC, 2007, 2009).

A mix of elevation data has been used for floodplain mapping. Detailed studies in high flood risk areas (main rivers and stream channels) used four foot contours from land surveying (NRC, 2009). Approximate studies in lower risk areas used USGS digital elevation models (DEMs), a gridded raster representation of a digital terrain model (DTM), derived from vector contour data (NRC, 2009). Due to land surveying costs, FEMAs Flood Map Modernization Program primarily uses land surface elevation data from mapped sources (NRC, 2007). While select U.S states have acquired or are in the process of acquiring state-wide higher resolution mapped LiDAR data coverage, most states still rely on U.S. Geological Survey (USGS) mapped (DEM) data generated from high altitude photography.

1

These elevation data have three inherent deficiencies; an average age of 35 years old, needed land features are not captured by the 30 meter point spacing, and an absolute elevation error in meters (NRC, 2009). To create accurate flood modeling and mapping, the U.S. NRC recommends establishing a nation-wide elevation dataset of high resolution light detection and ranging (LiDAR) elevation data (NRC, 2007). USGS and the National Digital Elevation Program have developed requirements for the U.S. National Enhanced Elevation Assessment (NEEA) (Dewberry, 2011). Additional research evaluating use of digital terrain models (DTMs), a bare-earth terrain representation generated from irregular spaces between points, could contribute to producing accurate flood models. In particular, a dearth of research exists for flood modeling in mountain environments.

Existing flood modeling research in mountain environments has focused on specific applications, such as, the influence of wildfires and the transport of solids on flood flows (Rulli & Rosso, 2007; Ruiz-Villanueva et al., 2014), flash flood forecasting (Tao & Barros, 2013), and glacial lake outburst floods (Westobsy et al., 2014; Worni et al., 2014). The U.S. NRC, through the North Carolina Floodplain Mapping Program (NCFMP), reviewed the effects of hydrologic, hydraulic, and elevation data on flood map accuracy for Ahoskie Creek in the Coastal Plain, Long Creek in the Piedmont, and the Swannanoa River in the Mountains of NC using high resolution LiDAR and USGS DEM data (NRC, 2009). Through the NCFMP studies, the U.S. NRC committee found that elevation data source was the most influential variable when determining flood extent, water surface elevation, and BFE calculations (NRC, 2009).

Colby and Dobson (2010) compared flood modeling results using different elevation data sources and spatial resolutions for two rivers located in North Carolina's Coastal Plain (Tar River) and Mountains (Watauga River). They compared flood modeling results using a series of LiDAR elevation data resolutions (6.1m, 15.2m, and 30m) and 30m USGS DEM data. The authors found that a 30m spatial resolution was unsuitable for flood modeling regardless of data source and up to a 15m LiDAR spatial resolution may be effective for flood modeling in a mountain environment.

This study addresses the effects of elevation data source and spatial resolution on flood modeling. This study sought to determine if an optimal resolution or range of resolutions for riverine flood modeling in a mountain environment exists. This study expanded on Colby and Dobson's study with the addition of numerous spatial resolutions, recurrence intervals, and diagnostic methods. Data sources included LiDAR data represented at a series of resolutions (3.77m, 6m, 8m, 10m, 12m, 15m, 20m, 25m, and 30m), and USGS DEM data at two resolutions (10m and 30m). Each elevation was combined with a series of flood recurrence intervals 10yr, 25yr, 50yr, 100yr, and 500yr for testing against a reference 3.77m LiDAR resolution A variety of descriptive and inferential statistics were used to evaluate water surface profiles (WSPs) and depth grids generated using the United States Army Corps of Engineers (USACE) Hydrologic Engineering Centers – River Analysis System (HEC-RAS) hydraulic model and Environmental Systems Research Institute's (ESRI) ArcGIS software.

Chapter 2

BACKGROUND AND LITERATURE REVIEW

2.1 Flood Insurance

Flood insurance provides the opportunity for property owners to purchase the coverage necessary to reduce the costs of hazardous flood events. Prior to 1968, flood insurance was provided by private insurance companies who could charge what they deemed as necessary to alleviate the costs incurred for potential flood events. Due to public outcry concerning unfair and unaffordable flood insurance, the government decided to make flood insurance affordable and available to the general public (Federal Emergency Management Agency (FEMA), 2002). To address the need for affordable flood insurance, the National Flood Insurance Act was created in 1968 (NRC, 2007). The National Flood Insurance Program (NFIP), administered by FEMA, was established by federal statute and provided subsidized 'federal flood insurance' in qualified local jurisdictions (NRC, 2009). The NFIP does not mandate flood insurance; however a bank may 'require' that the property owner obtain flood insurance as a condition of obtaining a mortgage loan (FEMA, 2002).

To avoid potential future flood damages, the NFIP began to regulate land development in floodplains (FEMA, 2002; NRC, 2007). Requiring specific construction standards for new construction within the 100 year floodplain allowed the NFIP to reduce flood risk for both owners and the community. These standards have estimated to save the NFIP one billion dollars annually (FEMA, 2002). Determining repetitive flood damages of two or more $1,000 losses within a ten year period also can reduce NFIP financial burdens.

One percent of flood insurance policies are repetitive losses yet account for 33% of all paid

losses (FEMA, 2002). Determining floodplain building damage can provide financial

justification for flood mitigation projects such as flood protection upgrades and building

demolition. Flood insurance can alleviate the cost associated with federal disaster assistance

when a flood event occurs. Flood insurance is determined through flood modeling and the

production of Flood Insurance Rate Maps (FIRMs).

2.2 Flood Insurance Rate Maps

Flood insurance is determined by the FIRM. Amount of flood risk associated with a

property is visually represented by a FIRM allowing insurance agencies to assign a cost to

the land owner for living within a hazardous flood zone. FIRMs are produced using available

elevation, hydraulic, and hydrologic data to generate water surface elevations, base flood

elevations, and flood extent (NRC, 2007). Most FIRMs are created using mapped sources

rather than accurate and costly elevation field surveying (Gesch, 2007; NRC, 2007). Prior to

the FEMA's Map Modernization Program, most FIRMs applied USGS digital elevation

models (DEMs) created through conversion of elevation contours depicted on a 1:24,000-

scale topographic map into a gridded cell format (Hodgson et al., 2005; NRC, 2007). A

majority of these topographic maps were created in the 1970's making descriptions of land

surface elevation for our nation over forty years old (NRC, 2009).

Many disastrous US floods occurred in the early 1990's culminating with an

impressive flood on the Mississippi River in 1993. This flood prompted the National

Insurance Reform Act of 1994. In 1997, FEMA decided to modernize the Floodplain

Mapping Program. In September 1999, Hurricane Dennis produced over 15 inches of inland rain in N.C. Two weeks later Hurricane Floyd hit North Carolina producing over 19 inches of inland rain causing the Tar River to crest to 12.7 meters, 7.3 meters above flood stage producing greater than a 500 year flood level (Bales et al., 2000). In North Carolina 35 people died from inland flooding with 57 total deaths attributed to Hurricane Floyd (Bales et al., 2000). Hurricane Floyd generated over $5.7 billion ($4 billion in 1999) of damages within NC and 9.8 billion (6.9 billion in 1999) of damages overall (Bales et al., 2000). This flood event opened the eyes of North Carolina government officials to floodplain mapping and management. On September 15th, 2000 NC became the first FEMA Cooperating Technical State in the nation. As a Cooperating Technical State, NC became the first state responsible for producing all of their own FIRMs.

2.3 Topographic Data

The Committee on FEMA Flood Maps recently published a report stating that "topographic data are the most important factor in determining…the accuracy of flood maps" (NRC, 2009, p 2). Concerns were raised in Congress about map data available for the ambitious task to update Flood Insurance Rate Maps (FIRMs) to Digital Flood Insurance Rate Maps (DFIRMs) required by the FEMA Flood Map Modernization Program. The NRC appointed the Committee on Floodplain Mapping Technologies to research potential technologies for acquiring elevation data for floodplain mapping (NRC, 2007). They concluded that FIRM generation using mapped sources was inadequate for floodplain mapping and that new DFIRMs using light detection and ranging (LiDAR) elevation data are

6

required for FEMA's new Flood Map Modernization Program (NRC, 2007). New DFIRMs require a two foot contour interval for flat areas and a four foot contour interval for hilly areas (NRC, 2007). The Committee on FEMA Flood Maps stated that uncertainties in the United States Geological Survey (USGS) National Elevation Dataset (NED) are 10 times greater than the new DFIRMs required by FEMA for floodplain mapping (NRC, 2009).

The Committee on Floodplain Mapping Technologies noted that further studies needed to be completed with USGS 10m and 30m NED data examining hydrologic, hydraulic, and elevation uncertainties in flood mapping (NRC, 2007). The NRC created a Committee on FEMA Flood Maps to study how hydrologic, hydraulic, and elevation data affect flood map accuracy, to determine the economic benefits of new more accurate floodplain maps, and to find ways to manage flood data (NRC, 2009). At the request of the Committee on FEMA Flood Maps, the North Carolina Floodplain Mapping Program (NCFMP) conducted three case studies in the Appalachian Mountains, Piedmont, and Coastal Plains of North Carolina concerning three main uncertainties in flood modeling identified by the NRC: hydrologic base flood discharge, water surface elevation hydraulics, and floodplain boundary mapping (NRC, 2009). The study performed in the Appalachian Mountains of North Carolina selected by the NCFMP was located on the Swannanoa River in Buncombe County.

Accuracy of land surface elevation data was a critical element in determining accuracy for base flood elevation visually represented in DFIRMs. Depictions of land surface defined by elevation data can determine velocity, direction, and depth of floods delineating

horizontal extent (hydrology) and vertical depth of flooding (hydraulics). The NCFMP evaluated hydrologic, hydraulic, and topographic data sources used for flood modeling for all three studies (NCFMP, 2008; NRC, 2009). Hydrologic studies showed that the most reliable method for defining peak flood discharges is to use flood frequency analysis of stream gauge records (NRC, 2009).

The NCFMP evaluated five hydraulic studies: detailed studies, NC detailed studies, national limited detailed studies, national approximate studies, and an approximate NED model using two topographic data sources: NC bare-earth LiDAR dataset and 30m USGS Level 2 DEMs. All hydraulic studies used NC bare-earth LiDAR dataset for topographic representation except the hydraulic study that used a 30m USGS Level 2 NED DEM (NCFMP, 2008; NRC, 2009). The NCFMP (2008) noted a significant difference in BFE when comparing hydraulic studies using LiDAR bare-earth data to the approximate NED study. BFE was "significantly more influenced" by data depicting land surface elevation (LiDAR or NED) than by "any variation of methods" used for calculating channel hydraulics (NRC, 2009, p 62). This evidence provided the foundation that "topographic data are the most important factor in determining water surface elevations, base flood elevation, and the extent of flooding and, thus, the accuracy of flood maps in riverine areas" (NRC, 2009, p 2).

2.4 Issues of Scale

The most accurate spatial resolution to use in flood modeling is depicted by the topography of the land. Zhang and Montegomery (1994) performed two flood modeling studies in the mountains of Oregon, on the Metteman Ridge, and in California, on the

Tennessee Valley. The Metteman Ridge watershed contained slopes of 30-40% and the Tennessee Valley watershed contained a range of 20-30% slopes (Zhang & Montegomery, 1994). As grid size increased, computed peak discharge increased. This led to a preferable DEM grid size of ten meters or less for the Tennessee Valley watershed and a DEM grid size of four meters for the Metteman Ridge watershed.

In a study by Vaze et al. (2010), it was determined that higher accuracy LiDAR data provided a more detailed flood extent than USGS NED data and improved the ability to extract hydrological features from a DEM. Changes in hydrological features depicted by differences in elevation data can result in different predicted flood elevations in a hydraulic model.

Raber et al. (2007) sought to uncover a relationship between LiDAR DEM nominal post-spacing and flood zone delineation via hydraulic modeling. The study area was located on Reedy Fork Creek in the Piedmont of NC Raber et al. used bare-earth LiDAR data decimated to 2.1m, 4.12m, 6.28m, 8.5m, and 10.8m equivalent post-spacing resolutions after removing non-ground points to produce a 100 year flood extent or discharge. They found that BFE did not statistically change over the post-spacing values tested; however flood zone boundary was sensitive to differences in post-spacing. They also determined that obtaining LiDAR data below a 4m post-spacing would be difficult to justify for flood modeling.

Omer et al. (2003) sought to reveal the impact of varied spatial resolutions on cross sections, hydraulic modeling results, and floodplain delineations. Their study area was located on Leith Creek in the Piedmont of NC. Omer et al. tested a series of filtered LiDAR

data sets (5.9m – 17.6m resolutions) with four discharge levels. Hydraulic modeling results including floodplain delineation remained uncompromised when applying up to a 9.5m LiDAR spatial resolution.

Colby and Dobson (2010) sought to determine the optimal spatial resolution for accurate flood modeling. They performed two studies; one on the Tar River in the Coastal Plains of NC and the other on the Watauga River in the Mountains of NC. Using clipped transects, an aerial photo of the Tar River displaying inundated flood area following Hurricane Floyd was compared to a HEC-RAS WSP produced using airborne 6.1m LiDAR bare-earth data. The mean percentage of clipped transects flooded on the aerial photograph matched clipped transects from the HEC-RAS WSP generated from airborne 6.1m LiDAR bare-earth data. A sign test was performed on the distances flooded along transects. It was found that 15.2m and 30 m LiDAR and 30m USGS DEM spatial resolutions were significantly different at a 90% confidence level when compared to the 6.1m LiDAR bare-earth reference layer. On the Watauga River, Colby and Dobson evaluated 6.1m, 15m, and 30m LiDAR spatial resolutions. It was found that 15m LiDAR presented no statistical difference for flood modeling on the Watauga River. Colby and Dobson indicated that 15m LiDAR may be a maximum threshold for DTM resolution used for flood modeling in a mountain environment. They also provided evidence proving that a 30m spatial resolution regardless of data source LiDAR or USGS Level 2 DEM produces floodplain maps unsuitable for flood modeling.

2.5 Diagnostic Methods

There is a lack of diagnostic methods available for horizontal and vertical accuracy assessment of flood modeling results. Flood modeling is typically based on overall flood height for a 100 year flood. Hydraulic modeling involves surveyed cross sectional cut lines creating a detailed map of the stream channel for a particular survey location. How high a flood will reach is depicted by the topography of the land. Few methods have been developed for determining the accuracy of the horizontal extent of flooding, because of incomplete spatial and temporal reference data (Colby& Dobson, 2010; Raber et al., 2007).

2.6 HAZUS-MH & HEC-FDA

Within the United States two models are currently used to assess flood damage cost; Hazard United States – Multi Hazard (HAZUS-MH) developed by FEMA and the Hydrologic Engineering Center Flood Damage Analysis (HEC-FDA) developed by the U.S. Army Corps of Engineers. A third spatial program, ArcGIS developed by ESRI, can also be used to model damages spatially. Each model was evaluated to determine effectiveness in damage estimate production.

HAZUS-MH software contains models for estimating loss from earthquakes, floods, and hurricanes. HAZUS-MH combines hazard analysis and loss estimation models to produce physical damages, economic loss, and social impacts for hazardous events. Within HAZUS-MH a flood hazard analysis can be performed at a Level 1 or a Level 2 analysis. A Level 1 analysis requires little user input and is to be used as a "screening" (Pine, 2009). The estimate from a Level 1 analysis requires user input topography and depth-frequency data.

HAZUS-MH then provides a set of pre-set regional regression equations based on hydrologic regions within each state to complete the flood modeling. Topography is delineated in the form of a DEM. Depth-frequency data can be found via three sources; FIRMs/DFIRMs, Q3 data showing the 100 year flood boundary or triangular approximation theory when the resolution of the available DEM is not good enough to accurately depict cross section geometry (Scawthorn et al. 2006). Performing a Level 2 flood hazard analysis using the flood information tool (FIT) in HEC-RAS provides greater accuracy for symbolizing river hazards. A Level 2 analysis requires a working knowledge of ArcGIS, HEC-RAS, and HEC-HMS as well as local knowledge of flood hazards. A comparison of a Level 1 and Level 2 analysis in the HAZUS-MH flood model was performed in Harris County, TX. It was found that the Level 1 analysis was quick and least costly, but the Level 2 analysis was considered more cost effective due to its reliable building damage and loss estimate results (Ding et al., 2008).

HEC-FDA estimates individual building flood damage through the integration of hydrologic engineering and an economic analysis that uses risk analysis procedures for the creation and evaluation of flood risk management plans. HEC-FDA estimates discharge frequencies, uncertainty in discharge exceedance probabilities, and damage-stage functions using a Monte Carlo simulation. A Monte Carlo simulation is a numerical analysis method that calculates the estimated cost of damage while accounting for uncertainty in the fundamental parameters needed to determine flood damage. HEC-FDA was designed to aid the USACE in performing risk analysis for flood risk management. Unlike HAZUS-MH, HEC-FDA requires all site data for the analysis to be entered by the user.

HEC-FDA requires study configuration data, WSP sets, exceedance probability functions, regulation inflow-outflow functions, stage discharge functions, levee data, damage categories, structure occupancy type data, structure modules, structure inventory data, and stage damage functions from the user for modeling. Study configuration data includes stream location, damage reaches, analysis years, and WSPs. Generation of HEC-RAS WSPs corresponding to 2yr, 10yr, 25yr, 50yr, 100yr, 200yr, and 500yr flood events are required to calculate damage cost estimates within HEC-FDA. The WSPs produce "discharge-probability functions, stage-discharge functions, and stage-damage functions" (Johnson 2000). Exceedance probability functions are the probability of exceeding a flood magnitude otherwise known as discharge/flow or stage. Regulations of discharge-probability (inflow-outflow) functions define a relationship between unregulated flow and regulated flow from dams and levees. Stage-discharge functions transform a discharge (flow) into a stage (depth) for damage calculations. Levee data includes the top of the levee stage, failure characteristics, and interior and exterior stages. Stage-damage functions apply a structure name, description, and price for categorization within a damage classification. Structure category occupancy types include structure, contents, a content to structure ratio, uncertainties in the first floor elevation, value ratios, and depth damage functions. Structure modules include the name, description, and its assignment to a plan and analysis year. The structures are grouped by unique attributes to be able to calculate combined stage-damage functions. Stage-damage functions then calculate direct economic damages caused by a range of flood events for the stream being studied.

A complicated damage estimate model is not warranted to evaluate building damage costs. ArcGIS and basic math can achieve the same goal of producing flood damage building replacement costs. Luino et al. (2009) performed a flood damage estimate study on the Boesio stream in Lombardy, Italy using ArcGIS Spatial Analyst extension. A DTM, water surface elevation, and polygon building shapefile were used to calculate flood damage estimates. All shapefiles were converted to raster format for grid operations. Flood depth grids were masked by building shapefiles producing grid cells containing flood depth within each building. Average difference between ground and road surfaces were compensated for by subtracting 0.2 meters from the building flood depth grids. Reclassification of the building flood depth grid based on stage damage curves produced a damage degree for each grid. Building values and damage degrees were combined through multiplication producing a grid of potential loss for every cell. Luino et al. then exported potential loss grid cells to calculate a loss value for each building.

HAZUS-MH is a powerful flood hazard damage assessment program for regional analysis. However, for this study, a Level 2 analysis using the FIT tool was required. At the time of this study the FIT tool created numerous complications involving data transfer from ArcGIS into HAZUS-MH. HAZUS-MH also aggregated the damage data at a block unit level. For this study an individual building level damage analysis was needed.

Requirements for HEC-FDA can be daunting for any user who does not work for the USACE. HEC-FDA excels at analyzing individual building flood damages. For this study Brown and Caldwell created a Structure Inventory Database within HEC-FDA. At the time

of this study, HEC-FDA produced runtime errors regarding study reach. HEC-FDA program aid was only provided to USACE employees and engineers working on USACE projects. While Brown and Caldwell used HEC-FDA for a more comprehensive flood damage analysis, they still had to import HEC-FDA exports back into ArcGIS for flood damage spatial representation. HEC-FDA, while great for engineers, may not be the best choice for a simple flood damage cost analysis.

ArcGIS provided a platform for spatial building depth damage analysis using a bare-earth LiDAR DEM, HEC-RAS depth grid exports, and a Structure Inventory Database (SID) file. The SID should include a shapefile of building polygons with associated building feature location, surveyed first floor elevation, surveyed level of adjacent grade, and building cost replacement values. ArcGIS allowed each building to be assessed individually for flood damage costs. ESRI also provides extensive ArcGIS online user help for all consumers. For this study ArcGIS and a methodology similar to Luino et al. (2009) was used.

Chapter 3

GEOGRAPHIC REGION

The Swannanoa River is located in western NC, and originates high in the southern Appalachian Mountains, passes through a flat area surrounded by mountains near Biltmore Village in Asheville, NC, and terminates at the confluence with the French Broad River. The Swannanoa River was selected for this study due to physical characteristics its location within a mountain environment and recorded significant levels of historical flooding that have occurred within the Swannanoa River watershed. The Swannanoa River study reach was selected based on its substantial vulnerable built environment located within the 100 year (100yr) floodplain and its detailed hydrologic model.

3.1 HAZUS-MH & HEC-FDA

The Swannanoa River watershed contains many unique physical characteristics for a mountainous river. Watershed physical characteristics that can intensify flooding include elevation, slope, size, shape, and geology. A river is considered mountain when the majority of its channel length has a gradient greater than 0.002 m/m, even if portions of its channel flow through lower gradient valleys (Whol, 2000). The section of the Swannanoa River modeled in this study has a gradient of 0.00178 m/m; however the entire length of the Swannanoa River has a steeper gradient of 0.00354 m/m (Table 1). The Swannanoa River watershed has an elevation range of 1,344 m (1,943 m – 599 m) (Table 1). Steep terrain and slopes within the Swannanoa River watershed create an environment for flash floods, a characteristic of mountainous rivers. As the Swannanoa River nears its outlet the terrain

changes from steep mountains to a unique flat bowl-shaped area. The section of Swannanoa

River examined in this study has a river reach 12km in length and begins at Tunnel Road

near the confluence with Christian Creek, passes through Biltmore Village, and ends at a

location halfway between Biltmore Village and the confluence with the French Broad River

in Buncombe County (Figure 3.1). USGS gauge (03451000) has a drainage area of 337km^2,

has been in operation for 86 years, and is located on the Swannanoa River at Biltmore

Village (Table 1; Asheville Field Office, 2004; USGS, 2015). The Biltmore Village gauge

average annual discharge is 4.51 m^3/sec (USGS 2015). North Fork (Burnette) Reservoir

(HUC 06010105070010) provides the main source of drinking water for the City of

Asheville as well as Buncombe County and is the located east of Asheville, NC in the upper

Swannanoa River watershed (Figure 3.2; Fox et al., 2008). Bee Tree Dam, located east of

Asheville, NC on a feeder creek in the upper Swannanoa River watershed, is currently used

to retain excess water. The unique physical characteristics of the Swannanoa River

watershed, including the substantial built environment, make it an excellent candidate for this

study.

3.2 Built Environment

The Swannanoa River watershed lies within the metropolitan area of the City of

Asheville, NC. The Swannanoa River's primary vulnerable built environment includes

Biltmore Village and a section of the City of Asheville near its confluence with the French

Broad River. I-40, a major US interstate, passes through the entire length of the watershed. A

population of approximately 40,000 people resides near the outlet of the Swannanoa River.

17

The upper reach of the Swannanoa River is primarily rural suburban. As the Swannanoa River reaches Biltmore Village the topography flattens into a bowl shaped suburban area creating a prime environment for flooding. The Swannanoa River became an area of interest in September of 2004 when the remnants of two back to back Hurricanes, Francis and Ivan, created extensive damage and destruction from riverine flooding.

Table 1. Physical Characteristics

Watershed Area	337 km^2 [a]
Watershed Elevation Maximum	1943 m [b]
Watershed Elevation Minimum	599 m [b]
Watershed Elevation Range	1344 m [b]
Watershed Mean Slope	17.46 ^{o} [b]
Swannanoa River Gradient	0.00354 m/m [b]
Study Reach Length	12 km [c]
Study Reach Gradient	0.00178 m/m [c]
Daily Average Flow (based on 85 years of data)	6.51 m^3/s [a]
Peak Recorded Flow (1940)	521 m^3/s [a]
Peak Estimated Flow (1791)	1133 m^3/s [a]
CSM – Daily Flow	1.209 [a]
CSM – Peak Recorded Flow	99.14 [a]
Gauge Datum above NGVD29	602.5 m [a]
Average Transect Distance Flooded	134.61 m [c]
Area Flooded / Meter of River Reach	245 m^2/m [c]

[a] Source - USGS, measured for the watershed draining to the Biltmore, NC gauge (USGS 03451000).
[b] Source - calculated using 6.1 m resolution LiDAR data.
[c] Source - calculated using 3.77 m bare-earth LiDAR data, and for the 100yr recurrence interval.
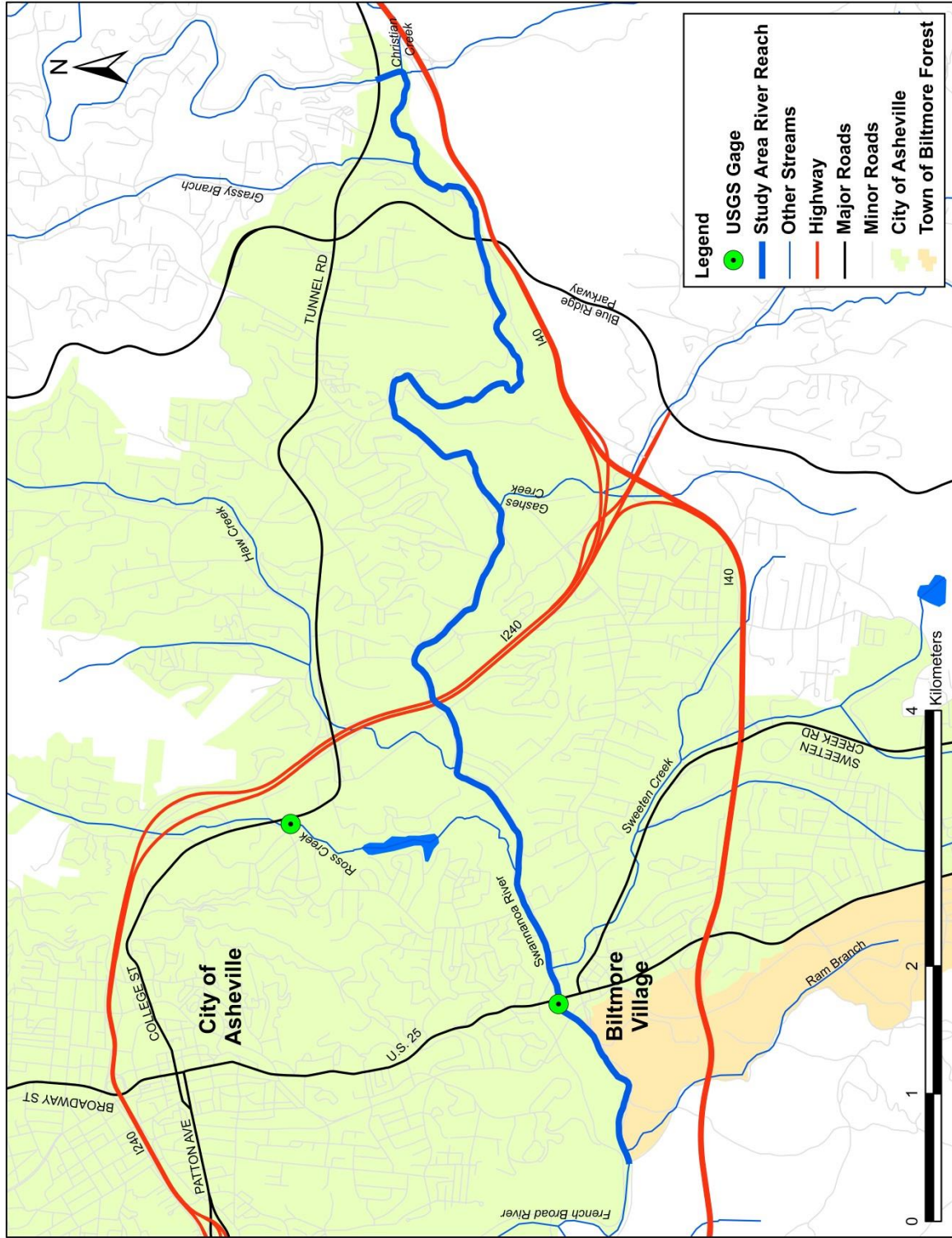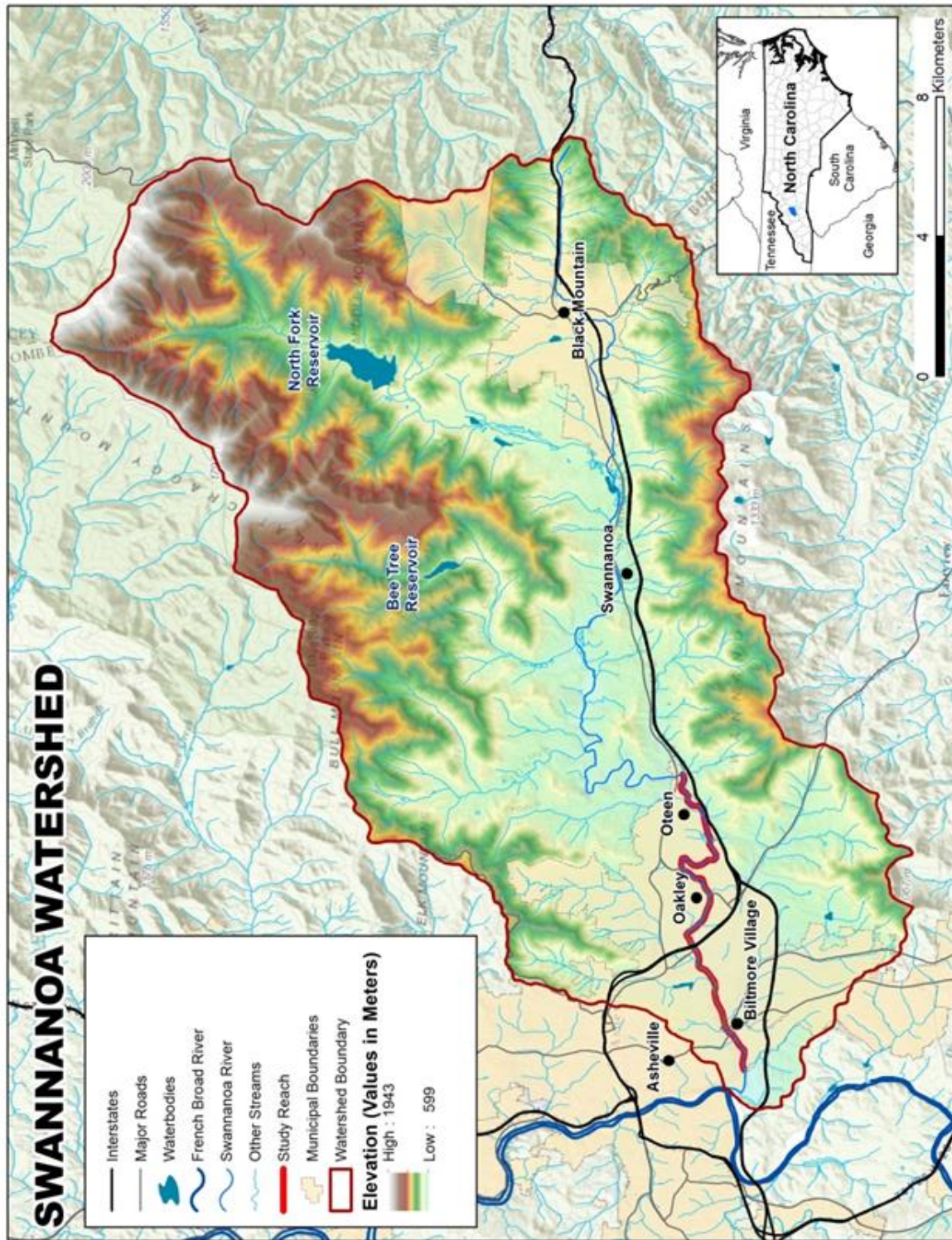
Figure 3.1. Swannanoa River Study Reach

Figure 3.2. Swannanoa River Watershed Map

3.3 Historical Flooding

Recorded significant levels of historical flooding have occurred on the Swannanoa River. Flood stage occurs when the Swannanoa River has crested over 3m in vertical height, moderate flood stage is categorized as over 4.4m, and over 5m is categorized as major flood stage as recorded at the Biltmore Village gage (National Weather Service, 2015). Since 1921, the Swannanoa River has experienced 20 recorded flood stage flows, of which 6 progressed to moderate flood stage flows, and 3 progressed to peak flood stage flows (USGS, 2015). From 1791 to 1916, the Swannanoa River has also experienced 12 estimated flood stage flows, of which 10 progressed to moderate flood stage flows, and 4 progressed to peak flood stage flows (USGS, 2015).

Two types of meteorological conditions tropical and extratropical precipitation systems cause meteorological floods in the Swannanoa River watershed. The high relief of the Appalachian Mountains can cause enhanced precipitation during meteorological events. Many of the major floods in the Swannanoa River watershed have been caused by tropical systems. In 1916, Swannanoa River flood waters reached 6.3m in vertical height flooding the neighborhood of Biltmore Village and the entire lower section of the City of Asheville, NC (USGS 2015). The 1916 flood on the Swannanoa River would have caused 62 million dollars in damages in 2010 (Brown & Caldwell, 2010). In 1928, Swannanoa River flood waters reached 5.7m in vertical height. Due to new industry in the area damages were nearly equal to those incurred during the 1916 flood (Brown & Caldwell, 2010).

In 2004, back to back tropical meteorological events, Hurricanes Francis (8 September) and Ivan (17 September) generated flood stages of 5.9m and 5.1m in vertical height respectively (Asheville Field Office 2004, USGS 2015). In a study performed by the USACE in 2005, it was found that $21.9 million in damages occurred to 116 commercial businesses located within the Swannanoa River floodplain (URS Group 2006). Total cost incurred far exceeded this amount estimated in to the tens of millions, which did not include residential structures, job, tourism, business, and agricultural losses. Many rivers and floodplains in the region experienced 500 year flood events from the back to back heavy rainfall events generated by Hurricanes Francis and Ivan. Combined these two hurricanes produced over $44 million dollars in damages within the state of North Carolina (FEMA 2004). Many people incurring flood damages did not have flood insurance due to a lack of knowledge that flooding occurred in their area. Noticing that residents were at risk for losing their businesses, jobs, and way of life, the President of the United States declared two federal disasters for western North Carolina (Basnight et al., 2005). This declaration provided needed aid from the U.S. Savings Reserve to North Carolina's Disaster Relief Reserve Fund in the amount of $123,541,447 to rebuild and revive western North Carolina after this substantial disaster (Basnight et al., 2005).

Swannanoa River floods alone have produced an estimated 675 million dollars in damages since 1901 (Brown & Caldwell, 2010). As of 2010, in excess of $650 million in structures and their contents exist within the Swannanoa River floodplain (Ormond, 2010). If a 100 year flood were to occur in 2010, over $79 million in direct damages would occur

(Brown & Caldwell, 2010). Rapid development in the built environment near the outlet of the Swannanoa River has made the Swannanoa River more susceptible to flooding. Accurate and precise flood models could aid officials in the thoughtful development of the built environment within the region. Unique physical, built, and historical characteristics make the Swannanoa River watershed an excellent candidate for this study.

Chapter 4

METHODOLOGY

4.1 Data Acquisition

Three components of data acquisition were essential to this study; elevation data, hydrologic/hydraulic data, and a SID. Elevation data consisted of two components LiDAR and USGS Level 2 DEM data. Hydrologic data was extracted from a detailed HEC-RAS model. A SID was obtained to calculate physical cost of flooding to structures located in the floodplain.

4.1.1 Elevation Data

LiDAR and USGS Level 2 DEM data were obtained and processed in different ways. LiDAR bare-earth data in the form of 3,048m x 3,048m (10,000ft x 10,000ft) tiles were downloaded from the NCFMP Flood Risk Information System. Buncombe County LiDAR data was acquired in 2005 from March thru April during leaf-off conditions by EarthData International, a subcontractor for Watershed Concepts. Bare-earth data was produced by removing all classified non-earth LiDAR points. Bare-earth data was saved in American Standard Code for Information Interchange (ASCII) format using North American Datum 1983 and North American Vertical Datum 1988. Six LiDAR bare-earth tiles with an average horizontal point spacing of 3.77m were downloaded for the Swannanoa River. Buncombe County LiDAR data vertical root-mean-square error (RMSE) equaled 25cm total with 17cm for open terrain, 24cm for weeds/crops, 35cm for scrub, 26cm for forest, and 18cm for built-up areas (NRC 2009). USGS Level 2 DEM 10 m and 30 m resolution data were obtained

from the USGS GIS Data Depot. USGS Level 2 DEMs were generated through a line-trace

contour-to-grid interpolation algorithm for digital line graph contours (Hodgson et al. 2005).

The U.S. NEEA has recognized 5 quality levels of elevation data (Dewberry, 2011; Snyder,

2012; Table 2). For this study, acquired LiDAR data fell between quality levels 3 and 4.

Table 2. U.S. National Enhanced Elevation Assessment Data Quality Levels

Quality Level	Horizontal Point Spacing (meters)	Vertical Accuracy (centimeters)
1	0.35	9.25
2	0.7	9.25
3	1-2	≤ 18.5
4	5	46-139
5	5	93-185

4.1.2   Hydrologic and Hydraulic Data

The reach of the river selected for this study contained a detailed HEC-RAS model

developed by Greenhorne and O'Mara (Raleigh, NC) and modified by Brown and Caldwell

(Charlotte, NC) for the NCFMP (NRC, 2007). A detailed study should encompass elevation

data obtained from LiDAR, field surveyed channel cross sections, defined ineffective flow

areas with channel obstructions such as bridges and culvert openings, and varying channel

Manning's "n" values (NRC, 2009). For this study, cross-sections were primarily manually

surveyed with supplemental cross-sections digitized on a Triangulated Irregular Network

(TIN) generated from bare-earth LiDAR to create the detailed HEC-RAS hydraulic model.

Hydrologic parameters were obtained from six USGS gauges; French Broad River at Bent

Creek, Hominy Creek in Chandler, Swannanoa River at Biltmore, French Broad River at

Asheville, NC, Beetree Creek near Swannanoa River, and North Fork of the Swannanoa

River near Black Mountain, NC (Table 3; NRC, 2009).

Table 3. Stream Gages Used for Flood Frequency Analysis

USGS Site	Site Name	Drainage Area	Years of Record
03448000	French Broad River at Bent Creek, NC	676	54
03448500	Hominy Creek at Candler, NC	79.8	37
03451000[a]	Swannanoa River at Biltmore, NC	130	78
03451500	French Broad River at Asheville, NC	945	85
03450000	Beetree Creek near Swannanoa, NC	5.46	72
03449000	North Fork Swannanoa River near Black Mountain, NC	23.8	32

[a] Locations of detailed flood hydrology and hydraulic studies.

At the request of the NCFMP, Brown and Caldwell modified this hydraulic model for

case studies in hydrology, hydraulics, and mapping. Bare-earth LiDAR data collected for the

NCFMP was applied by Greenhorne and O'Mara in the initial development of the detailed

level HEC-RAS hydraulic model. The same bare-earth LiDAR data was also applied by

Brown and Caldwell in the hydraulic model modification and used to generate the reference

TIN for this study. Discharge at the top of the study area reach and water surface level at the

bottom were extracted from the HEC-RAS model developed by Brown and Caldwell.

4.1.3 Structure Inventory Data

A SID containing residential, non-residential, and commercial structures located

within the 100yr floodplain and commercial structures located within the 500yr floodplain

was commissioned by the USACE and developed by Brown and Caldwell (Brown & Caldwell, 2010). The spatial SID developed for use within HEC-FDA software contained many features. Building feature location, surveyed first floor elevation (FFE), surveyed level of adjacent grade (LAG), and building cost replacement values were extracted from the SID for use in this study.

4.2 Data Processing

To compare flood modeling results using elevation from two sources (LiDAR and USGS), different pre-processing methods were required.. This study used a detailed HEC-RAS model to generate WSPs and depth grids for each equivalent elevation resolution and recurrence interval. Using the WSP with the greatest extent (3.77m LiDAR resolution at a 500yr recurrence interval) the SID was clipped leaving only buildings located within the study area.

Software used for this research included: ArcGIS produced by ESRI (Redlands, California), HEC-RAS and HEC-GeoRAS produced by the USACE Hydrologic Engineering Center (Davis, CA), and LiDAR Analyst (an extension for ArcGIS) produced by Textron Systems (Providence, RI).

4.2.1 Elevation Data

Within ArcGIS, six LiDAR ASCII tiles were converted to LASer (LAS) file format. LAS files were then converted and combined into a single multipoint shapefile. From the multipoint file within ArcGIS a TIN DTM file was generated. LiDAR bare-earth data was

decimated based on an area/point relationship in order to evaluate elevation models at different resolutions (Tobler, 1988):

$$d = \sqrt{\frac{A}{n}} \qquad (1)$$

where A represents the area, n represents the number of points, and d represents the average horizontal resolution. The Decimate TIN Node tool in ArcGIS was used to decimate the number of nodes to represent a series of equivalent resolution TINs. Original bare-earth data provided a 3.77m LiDAR equivalent resolution TIN. Original bare-earth data was decimated to create 6m, 8m, 10m, 12m, 15m, 20m, 25m, and 30m equivalent resolution TINs. Below, Figures 4.1, 4.2, and 4.4display examples of the 3.77m, 10m, and 30 m LiDAR equivalent resolution TINs respectively.

Two resolutions of USGS data were downloaded for this study. For most states within the U.S., standard elevation data sources are either a USGS 10m or 30m resolution DEM. For this study 10m and 30m spatial resolution USGS Level 2 DEMs were downloaded as tiles (10m (six tiles), 30m (one tile)) and mosaiced together. Each DEM was then converted to a TIN to be utilized within HEC-RAS to produce flood modeling outputs. Below, Figures 4.3 and 4.5 display examples of the 10m and 30 m USGS equivalent resolution TINs respectively.

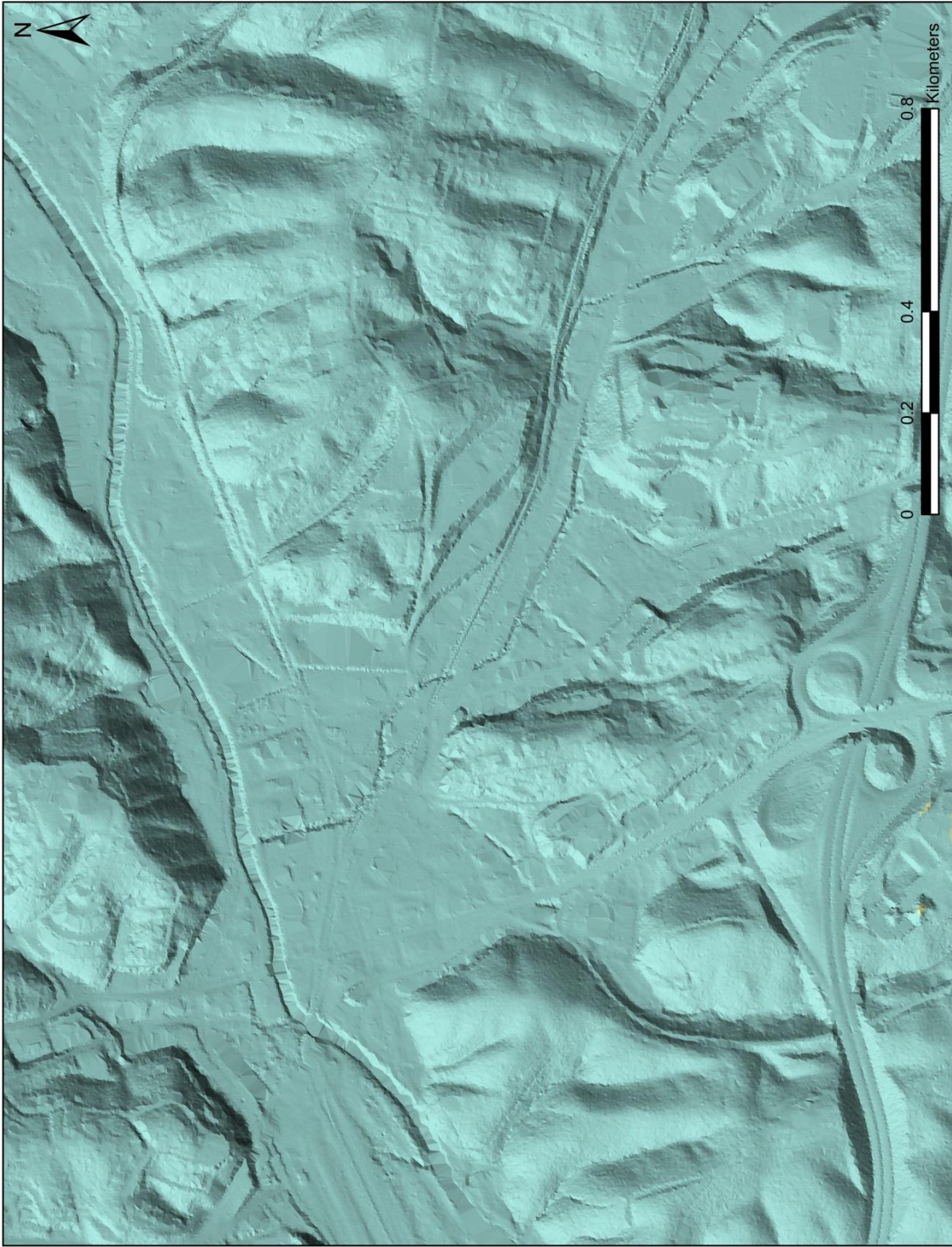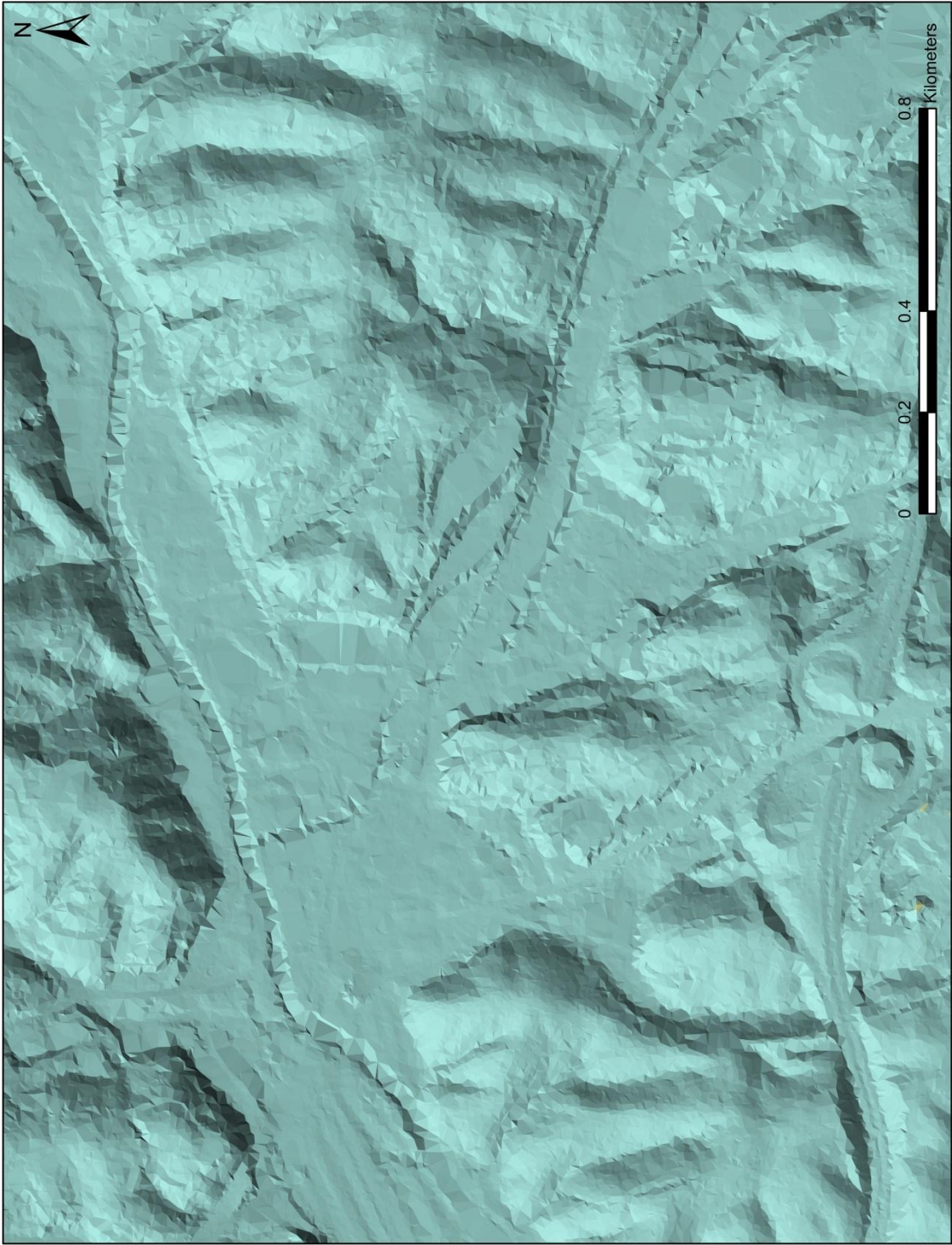**Figure 4.1.** Detailed View of Biltmore Village area on a 3.77m LiDAR TIN

Figure 4.2. Detailed View of Biltmore Village area on a 10m LiDAR TIN

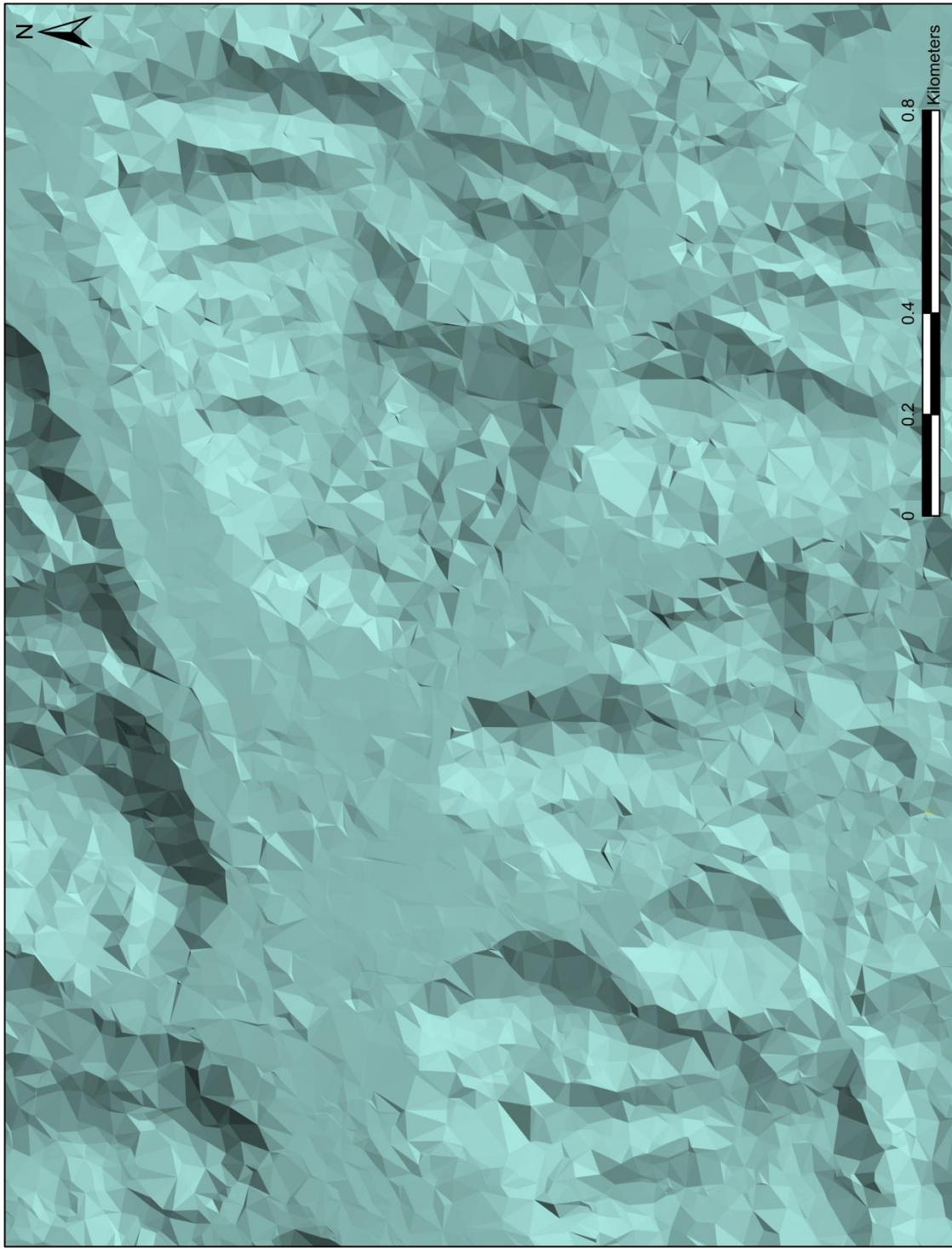**Figure 4.3.** Detailed View of Biltmore Village area on a 10m USGS TIN

31

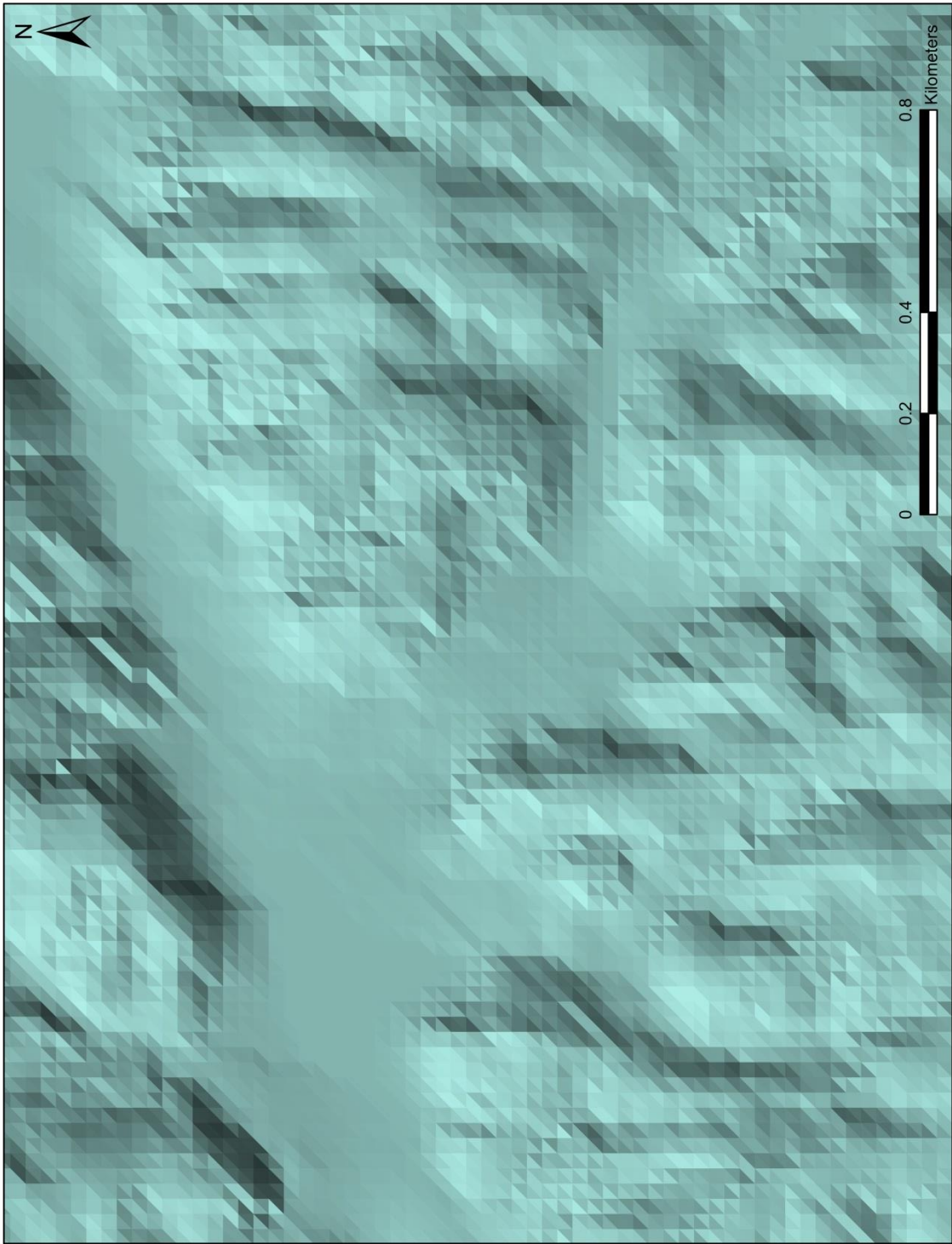**Figure 4.4.** Detailed View of Biltmore Village area on a 30m LiDAR TIN

Figure 4.5. Detailed View of Biltmore Village area on a 30m USGS TIN

4.2.2 Hydraulic Modeling

This study used the same detailed HEC-RAS model, developed by Greenhorne and O'Mara and modified by Brown and Caldwell for the NCFMP, to generate WSPs and depth grids for each equivalent elevation resolution and recurrence interval. For the study area reach, WSPs were generated using a steady and subcritical flow analysis for the 10yr, 25yr, 50yr, 100yr, and 500yr recurrence intervals. Through the HEC-GeoRAS extension WSPs were exported into ArcGIS. The series of TINs created from LiDAR data and USGS DEM data were used to represent WSP for depth grid creation in ArcGIS. Conversion of the HEC-RAS export file to an xml file format occurred prior to importing the file into HEC-GeoRAS. For raster file generation, TIN equivalent resolutions were used in the HEC-GeoRAS Layer Setup dialog box. For a series of discharge levels (5) and a series of equivalent resolution TINs (LiDAR and USGS Level 2) (11) WSPs and depth grids were generated resulting in a combination of 55 flood modeling results (Table 4).

Table 4. Recurrence Intervals and Equivalent Resolution TINs

Recurrence Intervals	LiDAR TINs	USGS TINs
10 year	3.77 meter	10 meter
25 year	6 meter	30 meter
50 year	8 meter	
100 year	10 meter	
500 year	12 meter	
	15 meter	
	20 meter	
	25 meter	
	30 meter	

4.2.3 Structure Inventory Data

In 2005, as a part of the Swannanoa Flood Risk Management Project, the USACE Institute of Water Resources hired Brown and Caldwell to create a Structure Inventory Database containing a plethora of economic data. The SID file contained 1044 residential and non-residential structures located within the 100yr floodplain (Brown & Caldwell, 2010). For this study building location, surveyed FFE, surveyed LAG, and building replacement value were extracted from the SID. In order to calculate cost damage estimates a simplified spatial SID, conversion of LiDAR TINs to raster based DEMs, and zonal statistics for each depth grid building footprint was needed.

The original SID contained structures for a greater extent of the Swannanoa River than the area being studied. Using the WSP with the greatest extent (3.77m LiDAR resolution at a 500yr recurrence interval) the SID was clipped leaving only buildings located within the study area. All equivalent resolution LiDAR TINs were converted to corresponding raster base DEMs using a natural neighbor resampling method in ArcGIS. Original mosaiced 10m and 30m USGS Level 2 raster DEMs were also used. Raster base elevations and depth grids were masked using the clipped SID buildings layer. In order to find the lowest point in the masked raster elevation file and the highest point in the masked depth grid for each building footprint, zonal statistics were calculated in ArcGIS. New minimum and maximum elevation values were added to the SID building layer. The building layer attribute table was then exported from ArcGIS into Microsoft Excel to calculate the total damage in dollars for each of the DTMs and recurrence interval pairs.

4.3 Diagnostic Procedures

Multiple diagnostic methods were used to evaluate the influence of elevation data on the representation of flood modeling results. All diagnostic methods used the 3.77m bare-earth LiDAR spatial resolution as the reference dataset. Diagnostic methods evaluated the WSPs and depth grids horizontally, vertically, and by volume.

4.3.1 Water Surface Profiles

Horizontal extent of WSPs were assessed using percent difference in WSP two-dimensional (2D) area, percent difference in symmetrical difference (SD) (area and shape), and distance flooded along transects drawn perpendicular to the river using inferential statistics. The following equation was used to calculate percent difference in WSP 2D area:

$$\text{Error } (\%) = \frac{Area(Poly) - Area(RefPoly)}{Area(REFPoly)} * 100 \qquad (2)$$

where Area(Poly) represents the area of the WSP polygon being evaluated and Area(REFPoly) represents the area of the reference WSP polygon.

Difference in both area and shape were determined using percent difference in SD. SD calculates the area where two polygons do not intersect, otherwise known as the complement in Boolean algebra. For this study percent difference in SD was calculated using the following equation (Gueudot et al., 2004; Colby & Dobson, 2010):

$$\text{Error } (\%) = \frac{Area(Poly) + Area(REFPoly) - 2*Area\,(Poly \cap REFPoly)}{Area(REFPoly)} * 100 \qquad (3)$$

where Area(Poly) represents the area of the WSP polygon being evaluated and Area(REFPoly) represents the area of the reference WSP polygon.

To evaluate the horizontal extent of WSPs, transects were drawn perpendicular to the stream centerline at stratified random locations (Colby & Dobson, 2010; Turner et al., 2013). For this study, twenty random transects were drawn within six equal segments along the river reach. Spacing of transects along the study reach averaged one transect per 100m. Length of original transects extended beyond the greatest extent of WSP flooding (3.77m 500yr). Transects were then overlaid, intersected, and clipped to WSPs (Figure 4.6).

Distances flooded along transects were measured for each WSP. Tests for normality were performed for each WSP dataset and found to be normally distributed. An inferential statistical paired t-test was performed to determine if a statistically significant difference existed between distances flooded along transects for the 3.77m WSP against distances flooded along transects for WSPs produced using generated TINs.
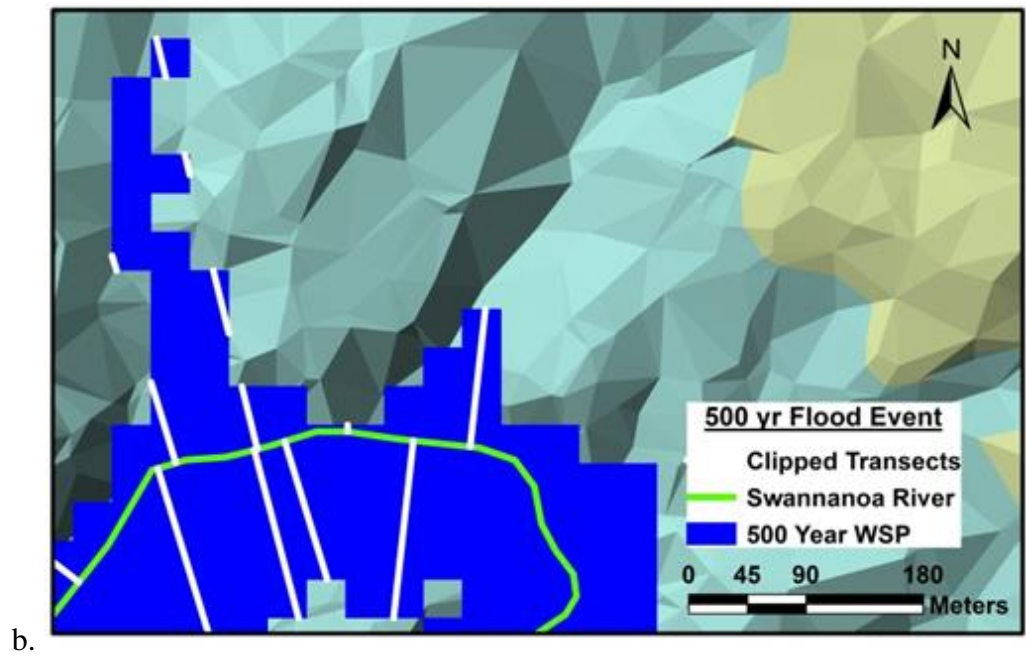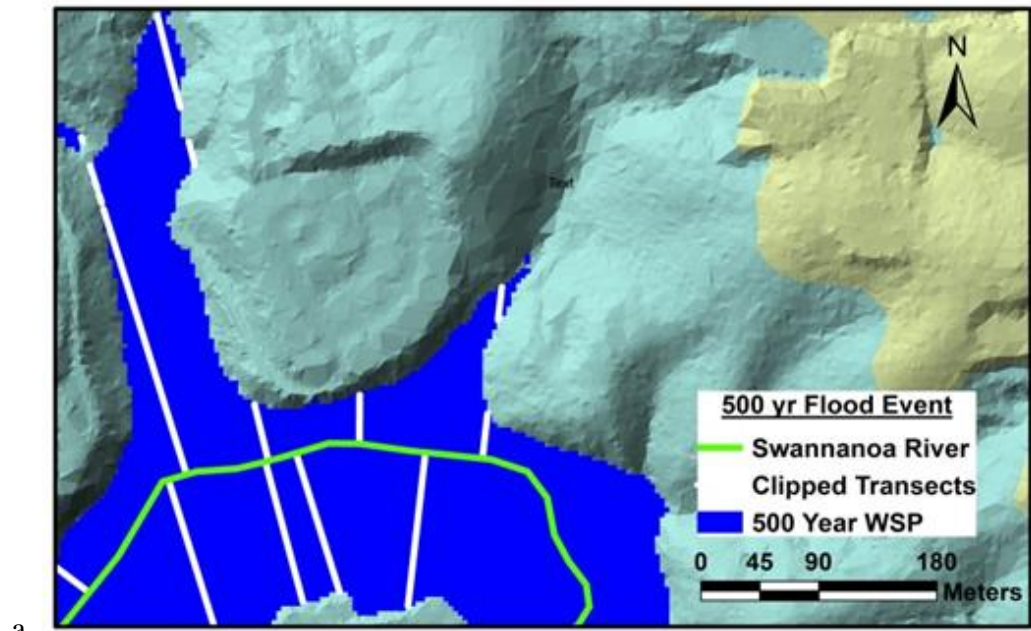
Figure 4.6. Transect lines drawn perpendicular to the stream centerline and intersected with the WSP generated using LiDAR TINs for a 500yr flood event: 3.77m equivalent resolution TIN (a), 30m equivalent resolution TIN (b).

4.3.2 Depth Grids

Depth grids were evaluated using descriptive statistics for maximum flood height, percent difference in volume, and RMSE. Maximum flood height was determined by comparing the maximum depth value for each depth grid to the maximum depth value for the 3.77m LiDAR depth grid. Volume was calculated using 3D Analyst in ArcGIS. The overall difference in volume was calculated using the following equation:

$$\text{Error } (\%) = \frac{Vol(DG) - Vol(REFDG)}{Vol(REFDG)} * 100 \qquad (4)$$

where Vol(DG) represents the volume of the depth grid being evaluated and Vol(REFDG) represents the volume of the reference depth grid.

The third depth grid diagnostic performed was RMSE. Within ArcMap all evaluation depth grids were masked and resampled to the reference 3.77m LiDAR spatial resolution. RMSE for each evaluation depth grid was calculated using the following equation:

$$\text{RMSE} = \sqrt{\frac{\Sigma(O-E)^2}{N}} \qquad (5)$$

where O represents the observed elevation value of the depth grid being evaluated, E represents the elevation value of the reference depth grid, and N represents the number of data.

4.3.3 Damage Estimates

Depth grids were also evaluated using a new method for calculating cost damage estimates. This method was similar to an approximate cost damage estimate method applied

by Luino et al. (2009). Damage estimates were calculated using the SID dataset, depth grids, and TINs.

To find the maximum flood depth above mean sea level for a building in the floodplain the depth grid maximum (measured in height above base elevation) and the base elevation minimum were added. Theoretically, elevation minimum in the raster base elevation file (not the basement) and the surveyed LAG should equal each other; however, this was rarely the case due to the varied values provided by different elevation datasets. To account for the error, minimum base elevation was subtracted from surveyed LAG (Figure 4.7).
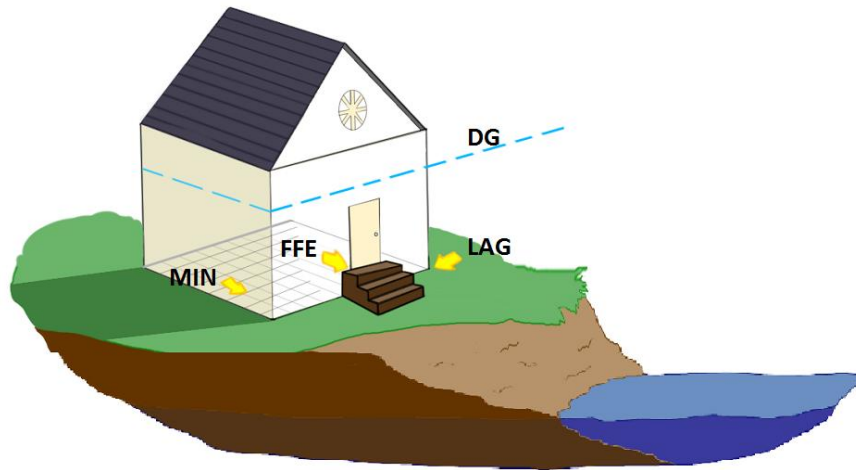

Figure 4.7. Depiction of raster depth grid maximum (DG), raster base elevation minimum (MIN), surveyed level at ground (LAG), and surveyed first floor elevation (FFE).

To calculate maximum flood height above FFE for each building the surveyed FFE and difference in error (between the raster base elevation minimum and surveyed LAG) were

both subtracted from the maximum flood depth (raster depth grid maximum and raster base

elevation minimum) using the following equation:

$$\big((DG + MIN) - (MIN - LAG) - FFE\big) = flood\ height\ above\ or\ below\ FFE \quad (6)$$

where: DG represents raster depth grid maximum, MIN represents raster base elevation

minimum, LAG represents the surveyed level at ground, and FFE represents first floor

elevation. Resulting flood height above or below building FFE corresponds with a respective

mean damage percent in the USACE structure depth damage table (Johnson, 2000). FFE is

considered equal to a flood depth of zero on the USACE structure depth damage table (Table

5). Corresponding percent damage was multiplied by building replacement value and

summed for all buildings within each combination of equivalent resolution TINs and

recurrence flood intervals. Since the majority of structures within the 500yr floodplain were

single story with no basement the USACE structure depth damage table for one story

buildings with no basement (Table 5) were used to calculate mean percent of building

damage. Content damage as a percent of structure value was not included in the damage

estimates. Therefore, damage estimates calculated using this method would underestimate

total damage due to flooding. This approach for calculating damage estimates was not

intended to determine exact measurements of damage due to flooding, but rather to provide

approximate estimates for comparative purposes.

The USACE uses different depth damage tables for different types of buildings within

HEC-FDA. The study area contained 257 buildings total. Of the 257 buildings, 202 were

one-story tall, 5 were 1.5 stories tall, 48 were two stories tall, one was three stories tall, and

one was four stories tall. Only nine buildings of the 257 buildings contained a basement. The one-story with no basement table was chosen based on the large amount of commercial one-story buildings without basements located within the floodplain study reach (Dawson, 2003). The uniformity of the buildings within the study area negated the need for multiple depth damage tables. Damage estimates were used as a way to subjectively quantify how damage costs change with differing levels of spatial resolution. ArcGIS allows a user to create a flood damage model within a GIS allowing for 3D modeling of building damages.

Table 5. USACE Structure Depth-Damage Table

One Story, No Basement*	
Depth (meters)	Mean of Damage (percent)
-0.61	0%
-0.30	2.50%
0.00	13.40%
0.30	23.30%
0.61	32.10%
0.91	40.10%
1.22	47.10%
1.52	53.20%
1.83	58.60%
2.13	63.20%
2.44	67.20%
2.74	70.50%
3.05	73.20%
3.35	75.40%
3.66	77.20%
3.96	78.50%
4.27	79.50%
4.57	80.20%
4.88	80.70%

*Structure depth-damage table retrieved from Dawson (2003)

Chapter 5

RESULTS

5.1 Water Surface Profiles

WSPs were evaluated using a variety of diagnostics. Percent difference in 2D area was used to evaluate changes in horizontal area. Percent difference in SD aided in the evaluation of both area and shape which includes the area where two polygons do not intersect known as the complement in Boolean algebra. Inferential statistical analysis of distance flooded along transects drawn perpendicular to the river was the third diagnostic used to evaluate horizontal flood extent.

5.1.1 Percent Difference in Area

Percent difference in 2D area results for WSPs produced via LiDAR and USGS DEM data for a series of flood events are depicted in Figure 5.1b. Both USGS resolutions overestimated area flooded which was exlemplified at lower recurrence intervals. Both the 10m and 30m USGS resolutions for the 10 yr flood overestimated flooded areaby 25%. For a 100yr flood event at a 30m resolution, flooded area decreased by over 4% for LiDAR data and increased by over 5.5% for USGS DEM data. According to Figure 5.1a, there is an overall trend for LiDAR data to underestimate area flooded at lower recurrence intervals and at coarser resolutions. Notable decreases in LiDAR WSP area started at the 8m, 12m, and 20m resolutions. An overall decrease in area for the 8m, 12m, and 20m LiDAR resolutions of 0.2%, 0.9%, and 2.8% respectively occurred for the 100yr WSP flood event.
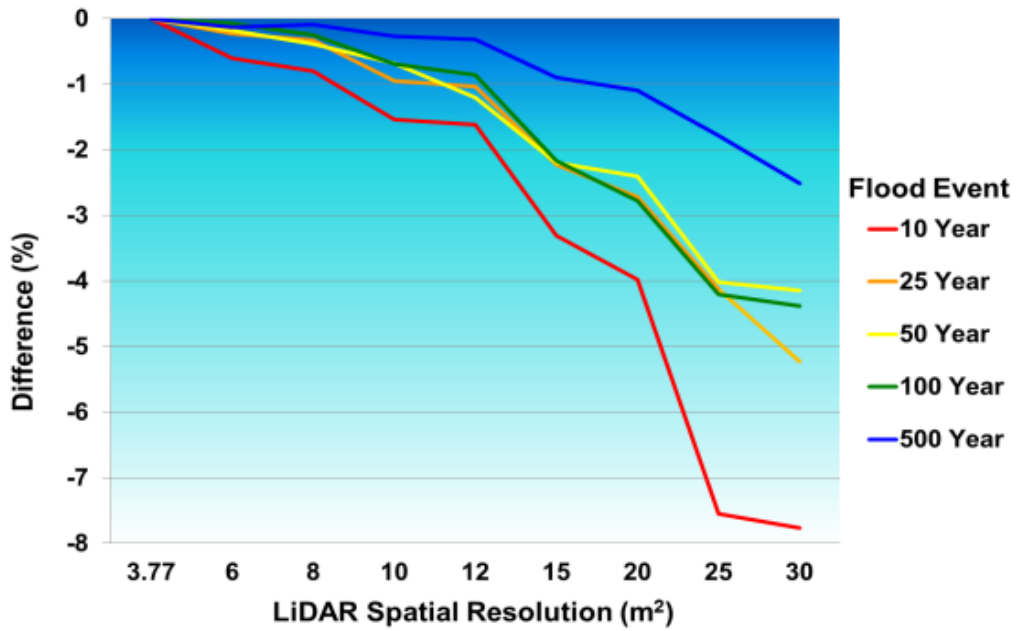
a.
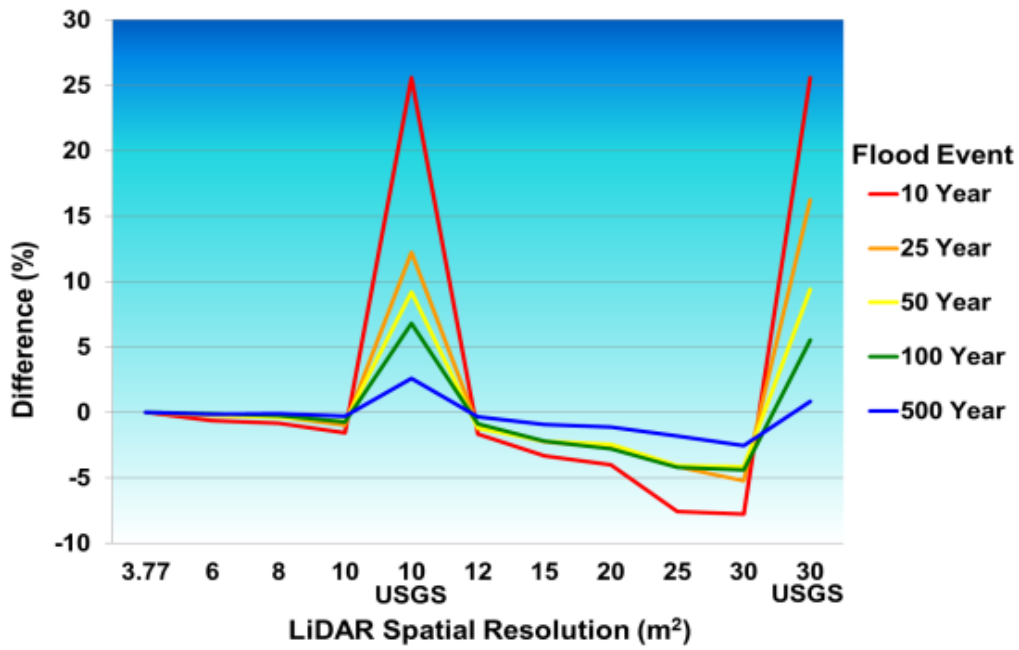
b.

Figure 5.1. Percent difference in 2D area for WSPs produced using LiDAR data (a) and for WSPs produced using LiDAR and USGS DEM data (b).

5.1.2 Percent Difference in Symmetrical Difference

Results from the analysis of percent difference in SD (area and shape) for WSPs

produced using LiDAR data for aseries of flood events are depicted in Figure 5.2. According

to Figure 5.2a, there is an overall trend towards a higher percent difference in SD (or

decrease in fit) at coarser LiDAR resolutions and for lower recurrence intervals. For a 100yr

flood event, over a 15% increase in percent difference in SD at the 30m resolution occurred.

A steady rise of percent difference in SD up to the 8m resolutionand after the 15m resolution

to the 25m resolution displays thresholds for flood accuracy based on perecent difference in

SD. Compared to the reference 3.77m LiDAR data for a 100yr WSP flood event, an increase

in percent difference in SD for the 8m and 15m LiDAR resolutions of 6% and 7.5%

respectively occurred. USGS data tended to overestimate area flooded for 10m and 30m

spatial resolutions and for lower recurrence intervals (Figure 5.2b). USGS data overestimated

10yr WSP flooded area by 30% for the 10m resolution and over 70% for the 30m resolutions.

For a 100yr flood event, area flooded at the 30m resolution increased by over 15% for
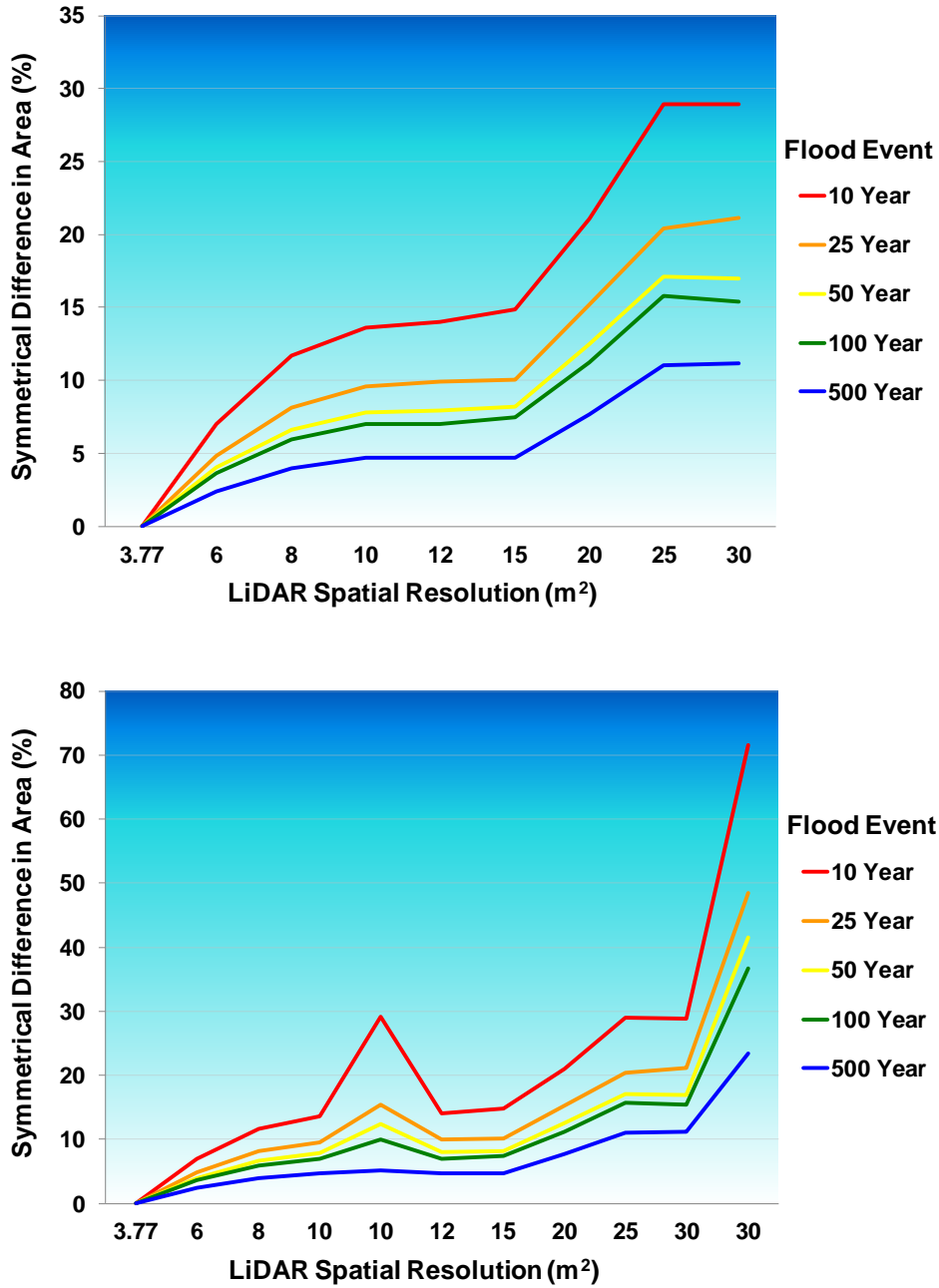
LiDAR data and 35% for USGS DEM data.

Figure 5.2. Percent difference in SD for WSPs produced using LiDAR data (a) and for depth grids produced using LiDAR and USGS DEM data (b).

5.1.3 Paired T-Test

Statistically significant results from the analysis of the inferential statistical paired *t*-test of flooded transect distance are depicted in Table 6. The null hypothesis stated that no difference in distance flooded along transects exists between transects clipped to the reference 3.77m LiDAR WSP and transects clipped to other generated spatial resolutions. According to Table 6, statistically significant LiDAR WSPs results (95% confidence interval) began at the 12m resolution for 10yr and 25yr flood events. Distance flooded along transects for WSPs produced using the 10m USGS DEM data were statistically significantly different for every recurrence interval. At the 100yr recurrence interval, distances flooded along transects intersected with WSPs produced using LiDAR data and 30m USGS DEM data were not statistically significantly different. Only the 10m USGS DEM WSP was stastically significantly different than the reference 3.77m LiDAR WSP at the 100 year recurrence interval.

Table 6. Paired T-Test for Distance Flooded Along Transects

| LiDAR Resolution	10 Year	25 Year	50 Year	100 Year	500 Year
6 m^2	0.47	0.33	0.39	0.37	0.35
8 m^2	0.26	0.77	0.63	0.52	0.62
10 m^2	0.09	0.13	0.13	0.17	0.36
10 m^2 USGS	0.00*	0.00*	0.00*	0.00*	0.04*
12 m^2	0.00*	0.03*	0.08	0.17	0.46
15 m^2	0.09	0.25	0.26	0.68	0.00*
20 m^2	0.01*	0.05*	0.27	0.85	0.18
25 m^2	0.01*	0.04*	0.02*	0.13	0.05*
30 m^2	0.10	0.03*	0.11	0.09	0.08
30 m^2 USGS	0.01*	0.05*	0.68	0.90	0.97

Significant at alpha = 0.05

5.2 Depth Grids

Four diagnostic results were performed for evaluating depth grids: maximum flood height, percent difference in volume, RMSE, and building damage estimates.

5.2.1 Maximum Flood Height

Results from the analysis of maximum flood height for depth grids produced using LiDAR and USGS DEM data for a series of flood events are depicted in Figure 5.3b. The 500yr flood event was not included in Figure 5a to better illustrate the differences in maximum flood height for the other recurrence intervals. According to Figure 5.3a, LiDAR data displays an overall trend to underestimate maximum flood height at coarser resolutions. Decrease amount for each flood event remains fairly consistent across LiDAR resolutions while USGS resolutions overestimated maximum flood height (Figure 5.3b). A 1.2m decrease in maximum flood height for30 m LiDAR depth grid occurred for the 100yr flood event. Conversely, a 7.1m increase in maximum flood height occurred for USGS depth grid data for the 100 year flood event. As shown in Figure 5.3a, notable decreases in maximum flood height started after the 8m and 15m resolutions occurred. Compared to the reference 3.77m LiDAR data for a 100yr flood event depth grid, a decrease in maximum flood height for the 8m and 15m LiDAR resolutions of 0.1m and 0.3m respectively occurred.
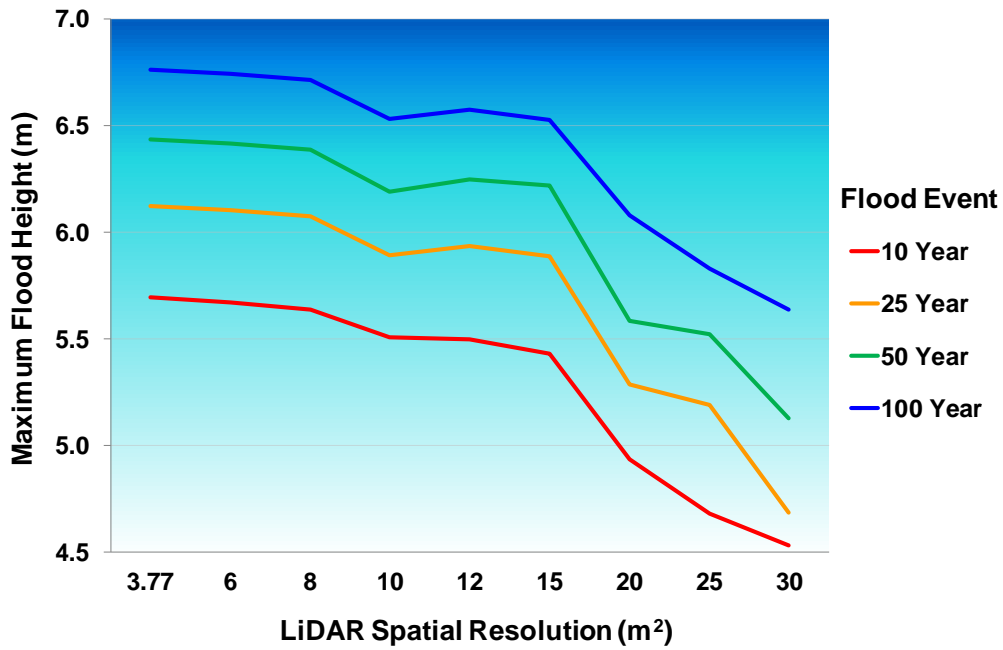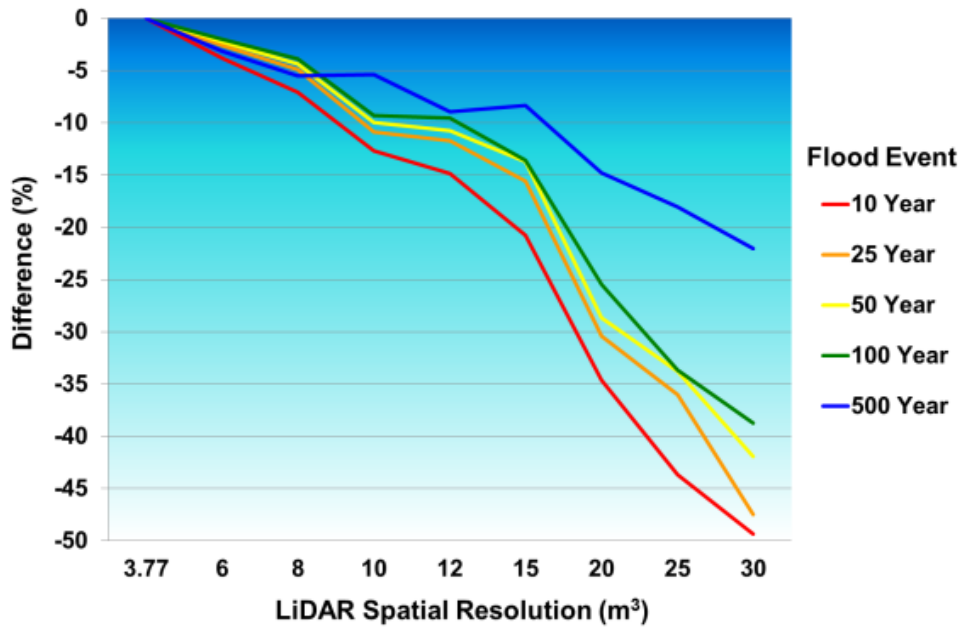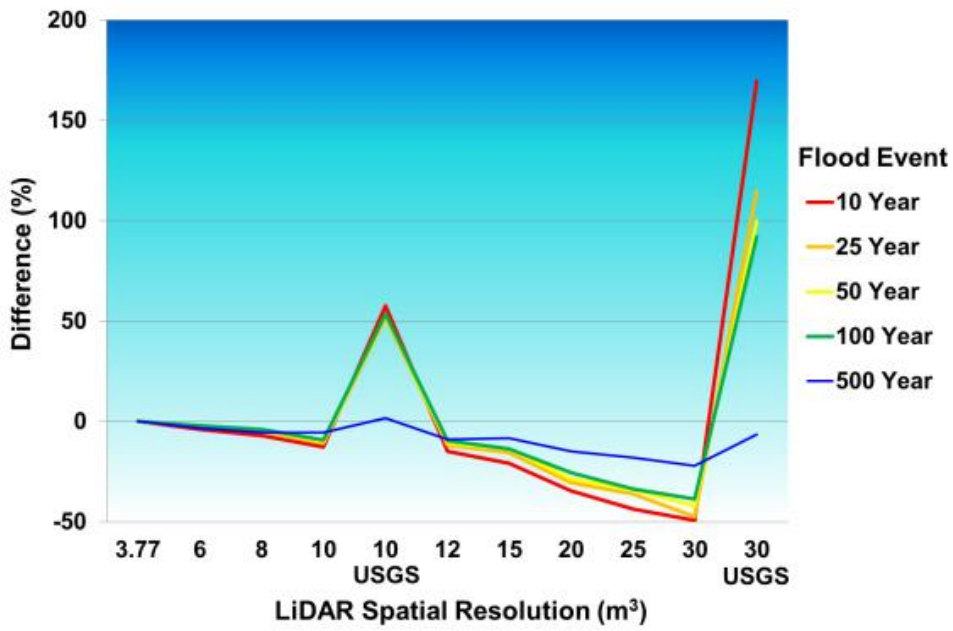
a.
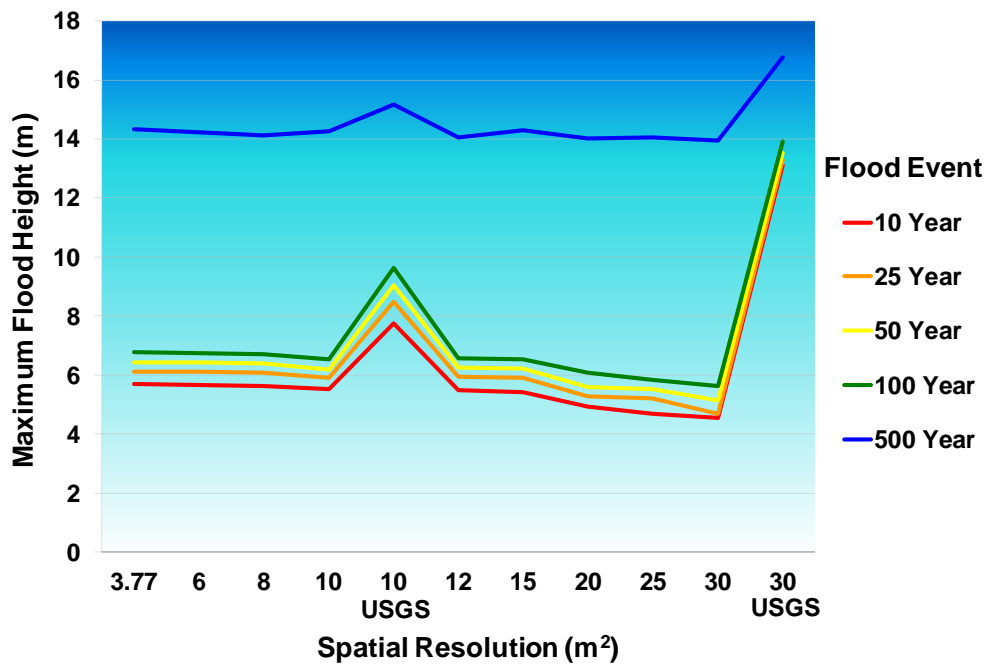
b.

Figure 5.3. Maximum flood height: for depth grids produced using LiDAR data (a) and for depth grids produced using LiDAR and USGS DEM data (b).

5.2.2 Percent Difference in Volume

Results from the analysis of percent difference in volume for depth grids produced using LiDAR and USGS DEM data for the series of flood events are depicted in Figure 5.4. According to Figure 5.4a, LiDAR data displays an overall trend to underestimate percent difference in volume at coarser resolutions and for lower flood events or recurrence intervals. USGS data tended to overestimate percent difference in volume at coarser resolutions and for lower recurrence intervals, although there is a decrease in percent difference in volume for the 500yr recurrence interval at the 30m resolution (Figure 5.4b). For a 100yr flood event, almost a 40% decrease in volume at the 30m resolution using LiDAR data and 90% increase using USGS DEM data occurred. In the graph comparing depth grids produced using LiDAR data (Figure 5.4a), general decreases in volume started after the 8m resolution and a more notable decrease starting after the 15m resolution occurred. Compared to the reference 3.77m LiDAR data for a 100yr flood event depth grid, there was a decrease in percent difference in volume for the 8m and 15m LiDAR resolutions of 3.9% and 13.6% respectively.

a.

b.

Figure 5.4. Percent difference in volume for depth grids generated using LiDAR data (a) and for depth grids produced using LiDAR and USGS DEM data (b).

5.2.3 Root Mean Squared Error

Results from the analysis of RMSE for depth grids produced using LiDAR data for the series of flood events are depicted in Figure 5.5. According to Figure 5.5, LiDAR data displays an overall trend towards increasing RMSE at coarser resolutions and for higher flood events or recurrence intervals. For a 100yr flood event there was over a 1m increase in RMSE at the 30m resolution. There appears to be a notable rise in RMSE for the 8m resolution and another increase after the 15m resolution. Compared to the reference 3.77m LiDAR data for a 100yr flood event depth grid, there was an increase in RMSE for the 8m and 15m LiDAR resolutions of 0.55m and 0.7m respectively. USGS data produced a notable rise in RMSE for both 10m and 30m resolutions and for higher recurrence intervals. Compared to the reference 3.77m LiDAR data for a 100yr flood event depth grid, USGS data displayed an increase in RMSE for the 10m and 30m resolutions of 0.86m and 2.69 m respectively (Figure 5.5b).
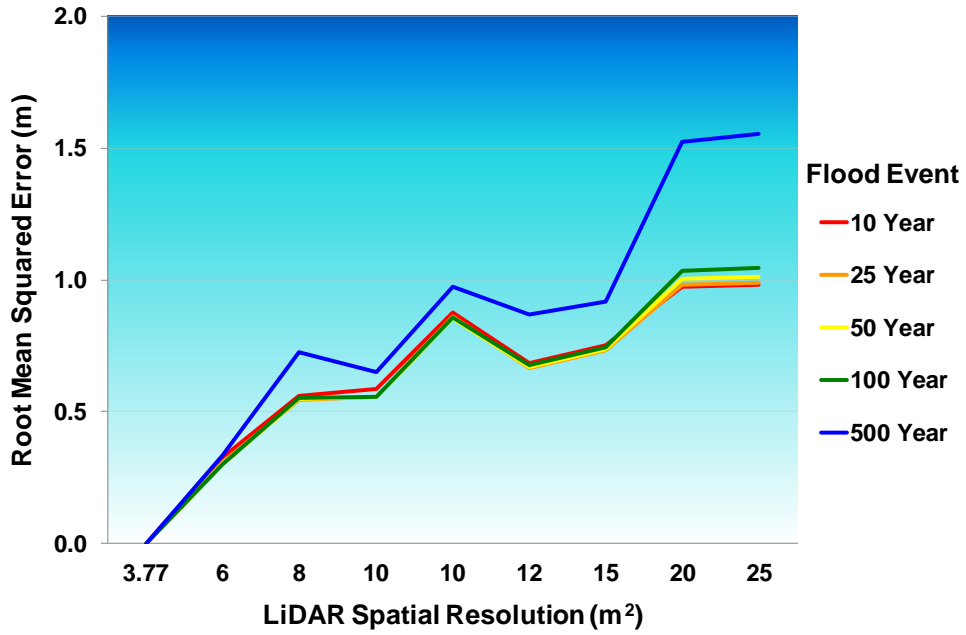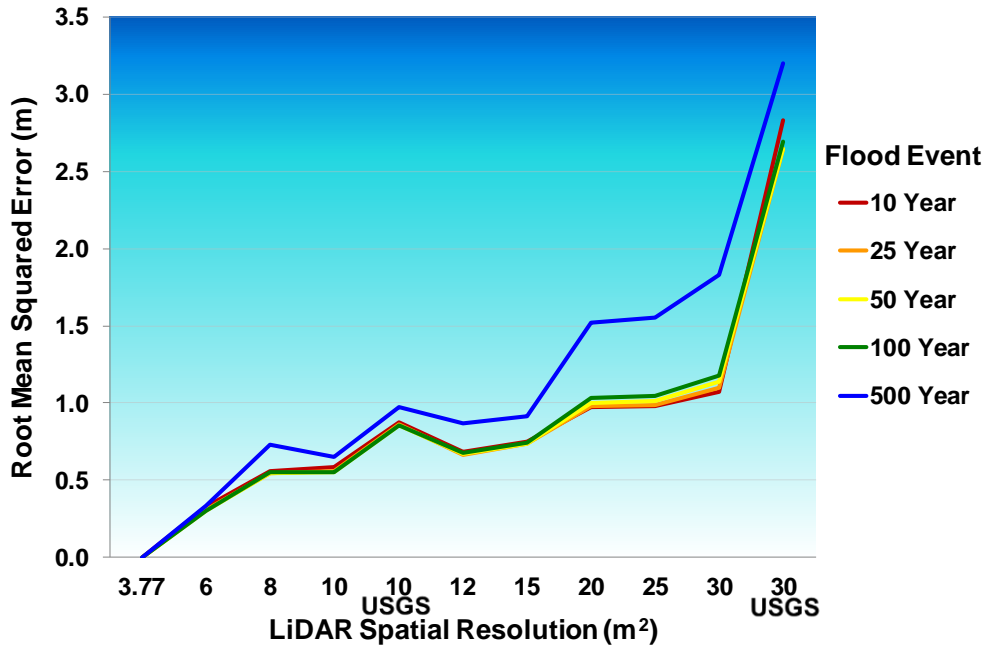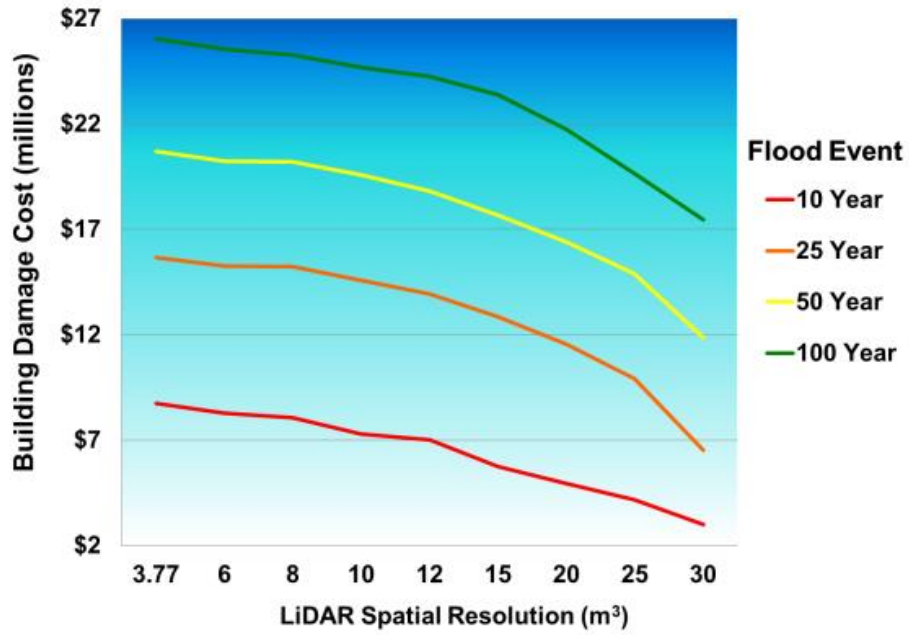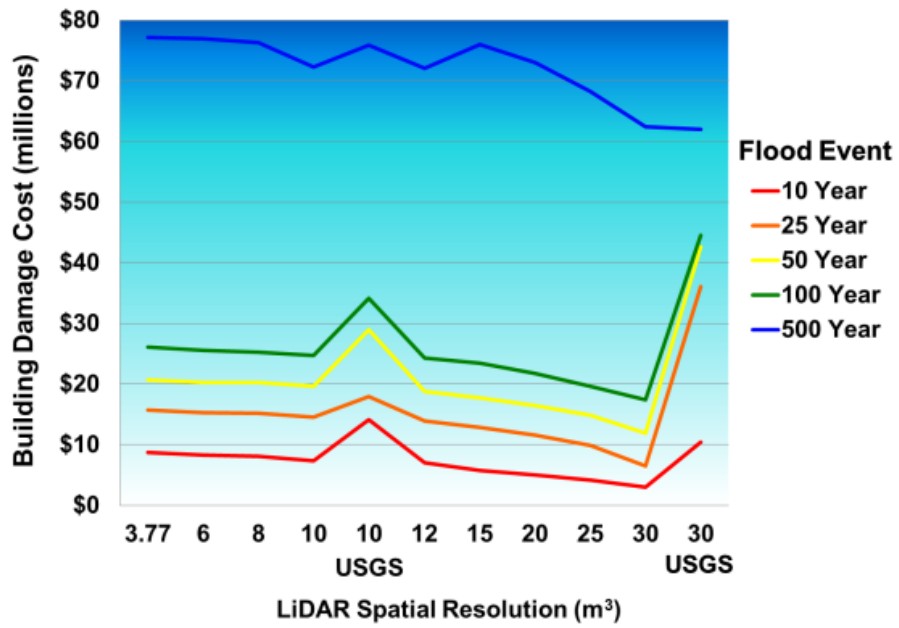
a.

b.

Figure 5.5. RMSE for depth grids generated using LiDAR data (a) and for depth grids produced using LiDAR and USGS DEM data (b).

55

5.2.4 Damage Estimates

Results for depth grid approximate building damage estimate analysis produced using LiDAR and USGS DEM data for a series of flood events are depicted in Figure 5.6. To better illustrate difference in building damage estimates for other recurrence intervals, the 500yr flood event is not included in Figure 5.6a. According to Figure 5.6a. LiDAR data displays an overall trend to underestimate building damage at coarser resolutions. This trend is also displayed in Figures 5.7, 5.8, and 5.10 where increasing LiDAR spatial resolutions underestimate flood depth. Amount of decrease for each flood event remains fairly consistent across resolutions. USGS data tended to overestimate building damage estimates at a coarser resolutions (Figure 5.6b), except for the 500yr flood event, displayed visually in Figures 5.9 and 5.11. A large amount of flooded area at a depth greater than 7m was diplayed in Figure 5.11 compared to the reference 3.77m LiDAR depth grid displayed in Figure 5.7. For a 100yr flood event, there was an approximate $8.5 million decrease in building damage estimates using the 30m LiDAR resolution and an approximate $18.5 million increase using the 30m USGS resolution as depicted in Figure 5.6b. LiDAR displays a fairly consistent downward trend in building damage estimates with a notable decrease occuring after the 15m resolution for the 100yr flood event in Figure 5.6a. Compared to the reference 3.77m LiDAR data for a 100yr flood event depth grid, a $2.7 million decrease in building damage estimates occurred using the 15m LiDAR resolution.

a.

b.

Figure 5.6. Building damage estimates in millions of dollars for depth grids produced using LiDAR data (a) and for depth grids produced using LiDAR and USGS DEM data (b).
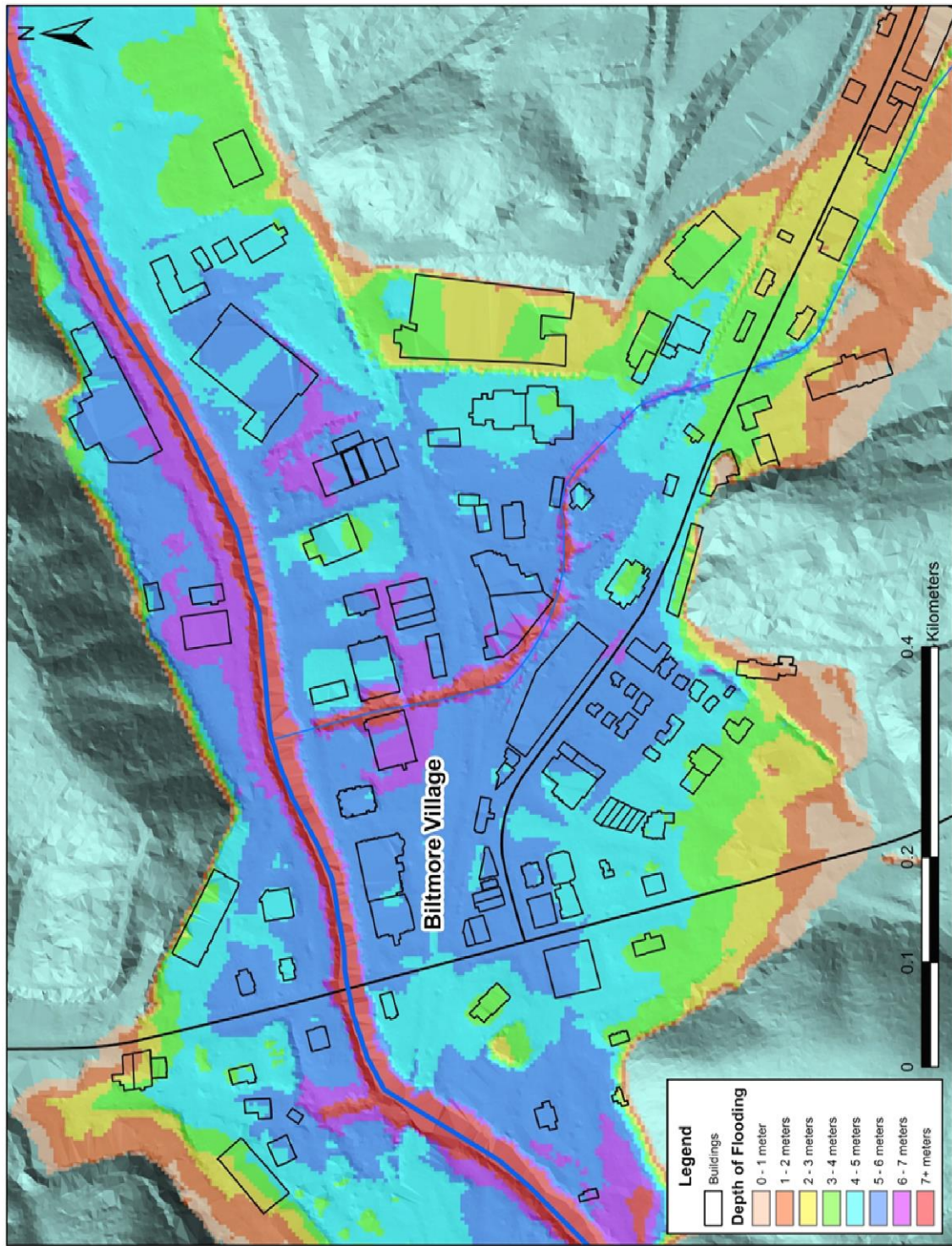
Figure 5.7. Detailed View of a 3.77m 500yr LiDAR depth grid of Biltmore Village buildings on a 3.77m LiDAR TIN.

Legend

Buildings

Depth of Flooding
0 - 1 meter
1 - 2 meters
2 - 3 meters
3 - 4 meters
4 - 5 meters
5 - 6 meters
6 - 7 meters
7+ meters

Biltmore Village

Kilometers

0   0.1   0.2   0.4

Figure 5.8. Detailed View of a 10m 500yr LiDAR depth grid of Biltmore Village buildings on a 10m LiDAR TIN.

Legend

Buildings
Depth of Flooding
0 - 1 meter
1 - 2 meters
2 - 3 meters
3 - 4 meters
4 - 5 meters
5 - 6 meters
6 - 7 meters
7 + meters

Biltmore Village

Kilometers

0   0.1   0.2   0.4

Figure 5.9. Detailed View of a 10m 500yr USGS depth grid of Biltmore Village buildings on a 10m USGS TIN.

Biltmore Village

N

Legend

Buildings

Depth of Flooding

0 - 1 meter
1 - 2 meters
2 - 3 meters
3 - 4 meters
4 - 5 meters
5 - 6 meters
6 - 7 meters
7 + meters

Kilometers
0.1   0.2   0.4

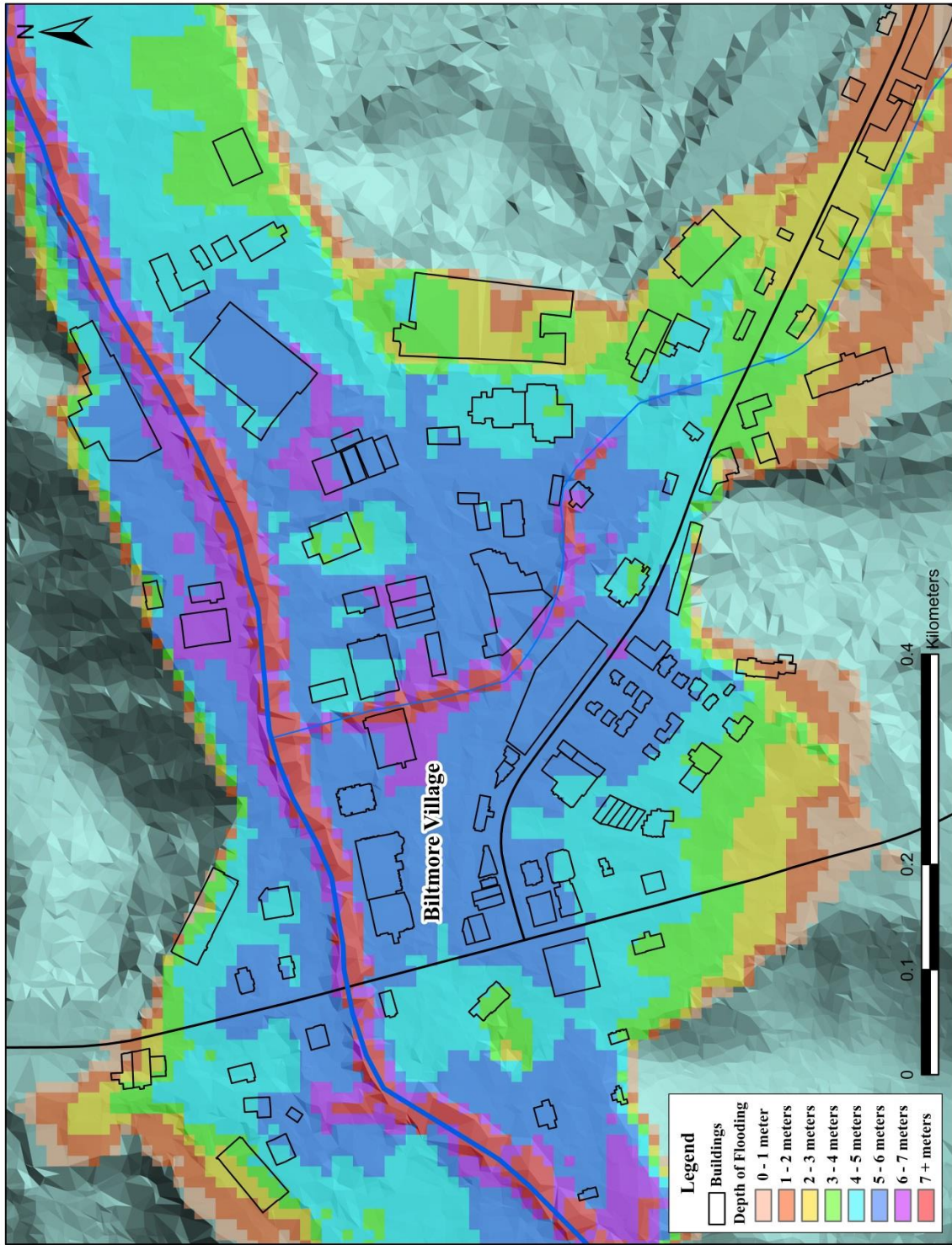**Figure 5.10.** Detailed View of a 30m 500yr LiDAR depth grid of Biltmore Village buildings on a 30m LiDAR TIN.

61

Figure 5.11. Detailed View of a 30m 500yr USGS depth grid of Biltmore Village buildings on a 30m USGS TIN.
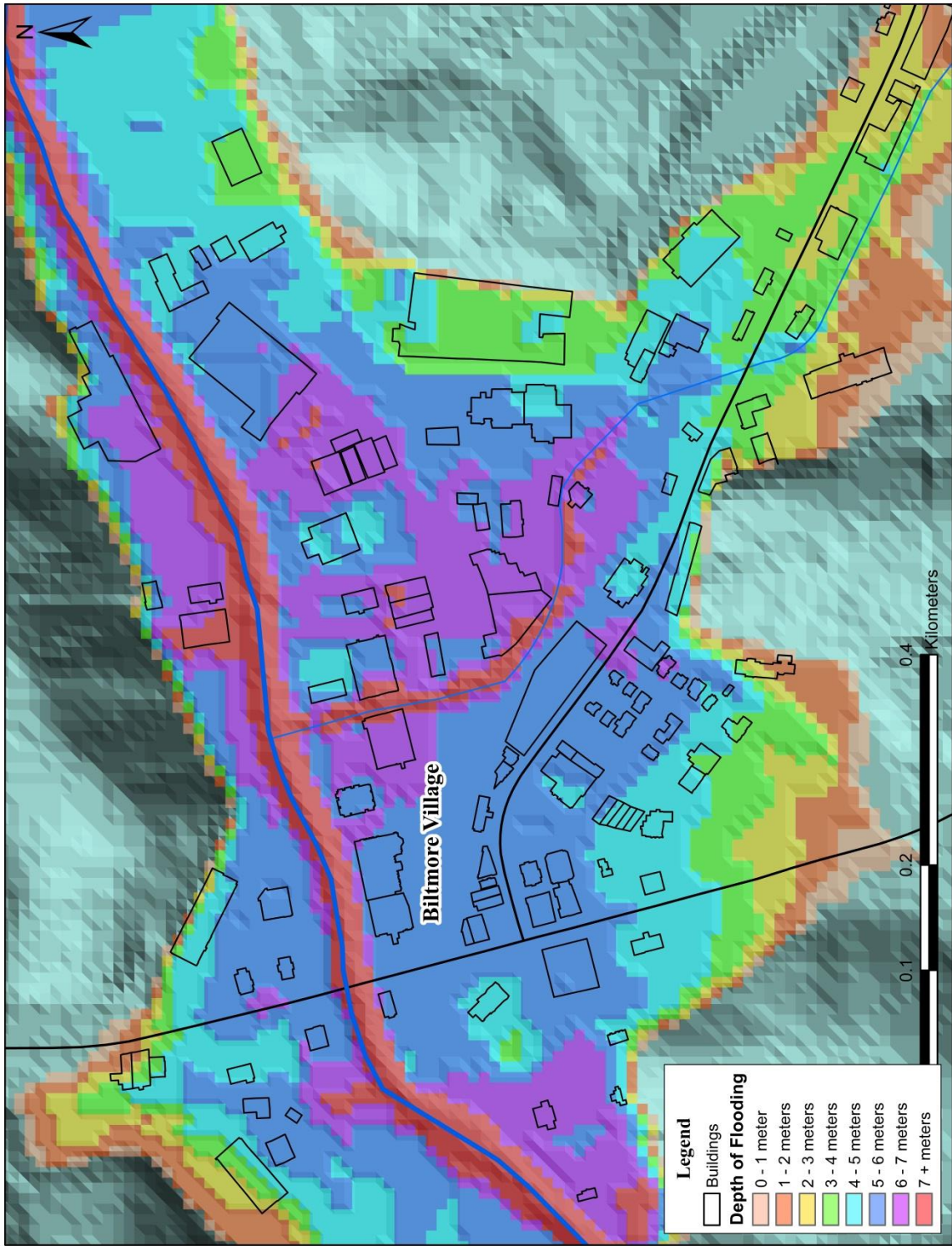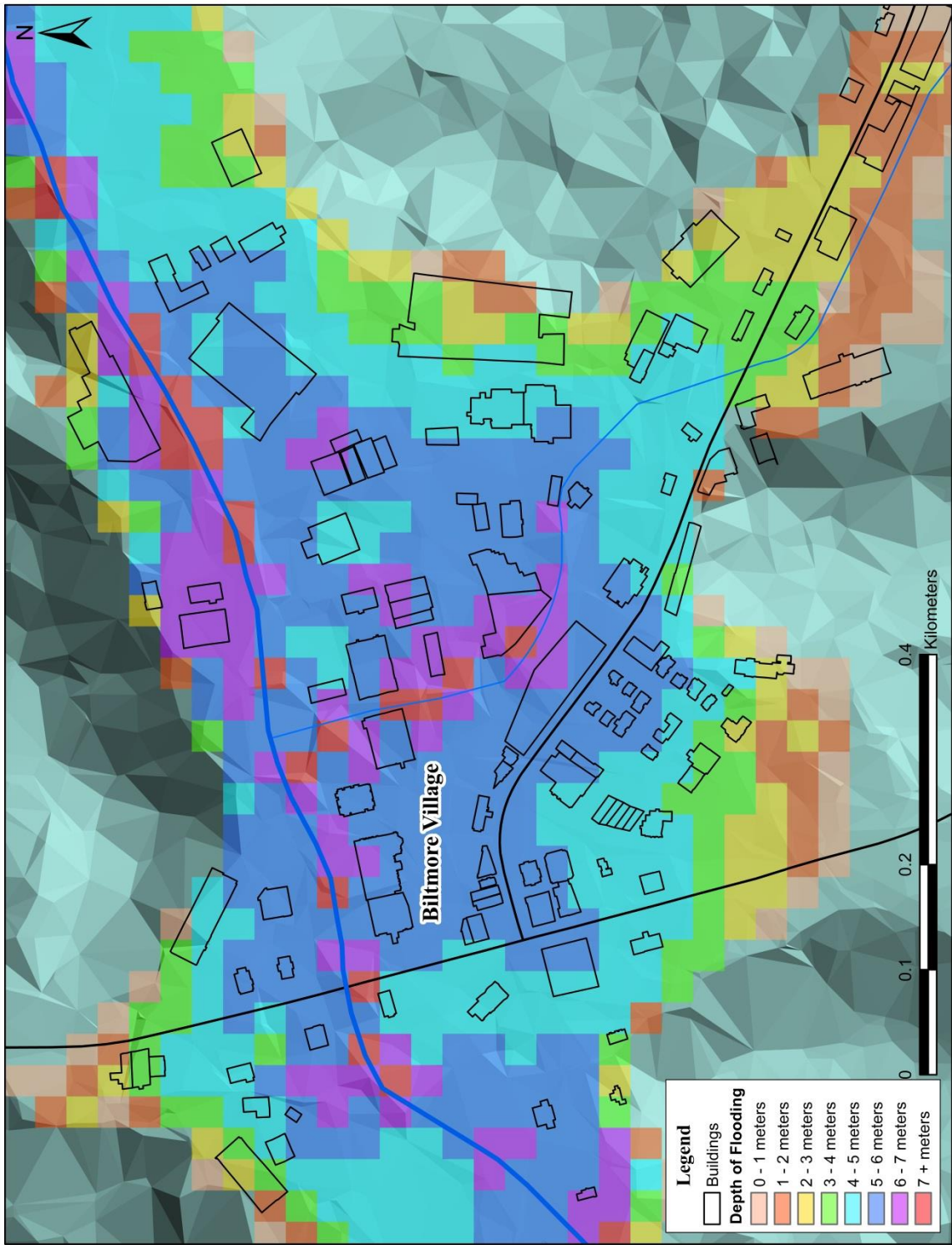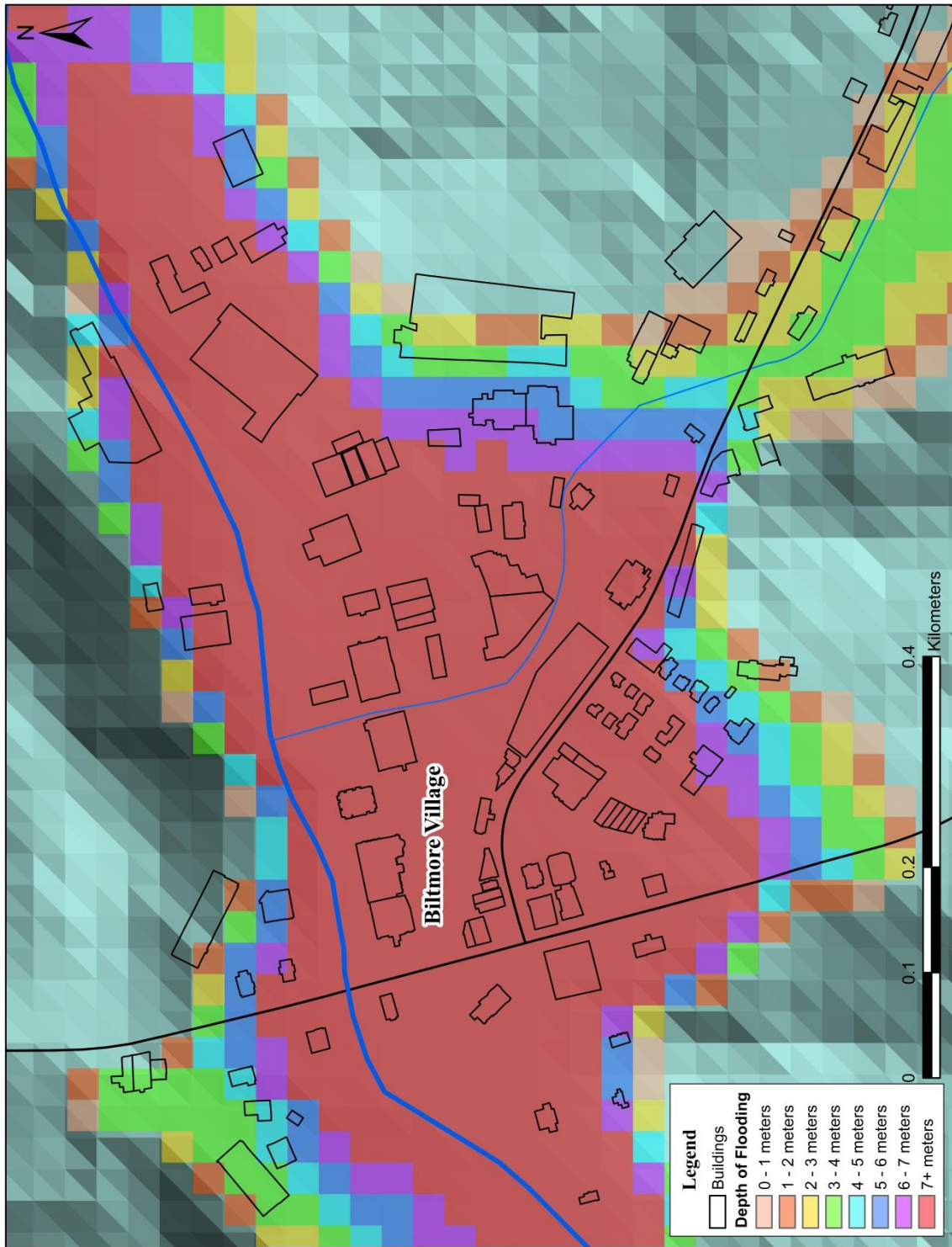
Biltmore Village

Legend
Buildings
Depth of Flooding
0 - 1 meters
1 - 2 meters
2 - 3 meters
3 - 4 meters
4 - 5 meters
5 - 6 meters
6 - 7 meters
7+ meters

Kilometers
0   0.1   0.2   0.4

Chapter 6

DISCUSSION

6.1 Trends

Upon reviewing the graphs of diagnostic results, a number of trends emerged. An underestimation occurred for LiDAR data at coarser resolutions and smaller flood events or recurrence intervals when analyzing the 2D area of WSPs and flood volume using depth grids. This trend is understandable as it would be more difficult to resolve flood extents and volumes for smaller recurrence intervals with coarser resolution data. An underestimation at coarser resolutions with generally similar differences for each recurrence interval occurred when analyzing depth grids for maximum flood height and building damage estimates. A decrease in flood depth is expected with lower recurrence intervals. An increase occurred at coarser resolutions and smaller recurrence intervals when analyzing the percent difference in SD of WSPs. An increase occurred at coarser resolutions and generally started at the 15m resolution for larger recurrence intervals when analyzing RMSE of depth grids. For these two diagnostic metrics an increase in error would tend to be expected at coarser resolutions and for smaller and larger recurrence intervals respectively. Results of the paired t-test were unique in terms of trends. The 10m LiDAR resolution was identified as the coarsest resolution for which the results were not found to be statistically significantly different for any recurrence interval.

Using the USGS data, an overestimation occurred for most diagnostic metrics rather than an underestimation. Overestimation occurred at a coarser resolution and for smaller

63

recurrence intervals when analyzing the 2D area of WSPs and flood volume using depth grids. When analyzing depth grids for maximum flood height, an overestimation occurred at a coarser resolution and for larger recurrence intervals. An overestimation at a coarser resolution occurred when analyzing depth grids for building damage estimates, except for the 10yr and 500yr recurrence intervals where there was a decrease at the 30m resolution. There was also a corresponding decrease in percent difference in volume for the 500yr recurrence interval for the 30m USGS DEM data. Results of the paired *t*-test indicated that the 30m USGS resolution performed better for large flood events than using the 10m USGS resolution.

As found by Colby and Dobson (2010), LiDAR data tended to underestimate and USGS DEM data tended to overestimate area and volume measurements when flood modeling in a mountain environment. Difference in results between data sources was attributed to coarser data resolutions lack of ability to capture terrain features in mountain environments resulting in differences in shape, extent, and location of generated WSPs and depth grids. Differences in data models may also play a role as elevation is represented at the original location of sample points in a LiDAR DTM; whereas USGS DEM elevation values are represented as the center point of grid cells in a 2D array, which may not represent terrain features as accurately.

Interestingly, at the 100yr recurrence interval, distances flooded along transects intersected with WSPs were found to be statistically significantly different for only the WSP produced using the 10m USGS DEM data. This result supports the inclusion of a series of

64

recurrence intervals when evaluating the influence of elevation data on flood modeling representation. No indication would have been provided that flood modeling results were sensitive to the representation of elevation at other recurrence intervals if only the 100yr recurrence interval was analyzed using this diagnostic metric.

6.2 Notable Breaks

Two resolutions tend to stand out when reviewing graphs of diagnostic results using LiDAR data. Breaks were noted at the 8m and 15m resolutions for five out of seven metrics. Calculating the difference in diagnostic results at these two resolutions can be useful in helping to determine whether an optimal resolution or range of resolutions can be identified for flood modeling in this mountain environment (Table 7). Overall large differences do not appear between results obtained for most diagnostic metrics at the 8m and 15m LiDAR resolutions. A case could be made for a useful range of resolutions existing through 15m for flood modeling, although a couple of values are worth mentioning. In regards to maximum flood height, 0.2m of flooded features created a $1.5 million dollar difference in building damage estimates which could be considered significant. In addition, for the best paired *t*-test results were obtained using 10m and finer LiDAR resolution data. Results from this research are similar to that found in other studies. For example, Colby and Dobson (2010) found that LiDAR data resolutions up to a 15m resolution may be useful for flood modeling in mountain environments and Omer et al. (2003) found that up to a 10 m LiDAR resolution could be used for flood modeling in the Piedmont of North Carolina.

Table 7. Difference in Diagnostic Results at 8m and 15m Resolutions

Diagnostic Method	8m	15m	Difference
% Difference 2D Area	0.2%	2.2%	2 %
% Symmetrical Difference	5.96%	7.45%	1.49%
Maximum Flood Height	6.7m	6.5m	-0.2m
% Difference in Volume	3.9%	13.6%	9.7%
Root Mean Square Error	0.55m	0.74m	0.19m
Building Damage Estimates	$25,256,362	$23,386,855	$1,869,507

Chapter 7

Conclusions

Determining the optimal elevation data for flood modeling in the creation of accurate digital flood insurance rate maps is critical (NRC, 2007, 2009). Using the finest resolution elevation data for flood modeling may be desired; however, identifying an optimal resolution or range of resolutions could result in a conservation of resources in terms of database development, maintenance, and analysis. Elevation data source is another key consideration for resource conservation. The U.S. NRC has recommended the use of LiDAR data for flood modeling; however, LiDAR data may not be widely available nationally and internationally. Within the U.S. many state-wide LiDAR datasets are still being developed; in addition, little research has been undertaken to determine the best elevation data to use for flood modeling in mountain environments. The objective of this research was to investigate whether an optimal resolution or range of resolutions of elevation data exists for flood modeling in a mountain environment using LiDAR and USGS DEM data for a series of flood recurrence intervals.

Findings from this research confirmed, as found in previous research, that USGS DEM data primarily produced lower quality flood modeling results in comparison to LiDAR data. Flood modeling results generated using 3.77m LiDAR data showed breaks in diagnostic results found most notably at the 8m and 15m resolutions. It could be argued that an optimal range of resolutions for flood modeling in this mountain environment could extend through the 15m LiDAR resolution; however, when reviewing maximum flood height and

approximate building damage estimates an optimal range of 8m LiDAR resolution or finer would be recommended.

Other findings from this research included use of a series of recurrence intervals and multiple diagnostic methods when evaluating elevation data representation for flood modeling. Results from this research were based on a sensitivity analysis using a reference LiDAR dataset categorized between U.S. NEEA Quality Levels 3 and 4. Further research could be pursued using higher resolutions of LiDAR elevation data (Quality Level 3 and lower) to determine if similar relationships exist between flood modeling results for a finer series of recurrence intervals (2 yr, 5 yr, and 200 yr) for rivers in mountain environments compared to flood extent and depth data gathered in the field.

Abbreviations

2D	Two Dimensional
ASCII	American Standard Code for Information Interchange
BFE	Base Flood Elevation
DEMs	Digital Elevation Models
DFIRM	Digital Flood Insurance Rate Map
DG	Depth Grid
DTMs	Digital Terrain Models
E	Expected
FEMA	Federal Emergency Management Agency
FFE	First Floor Elevation
FIRM	Flood Insurance Rate Map
HAZUS-MH	Hazard United States – Multi Hazard
HEC-FDA	Hydrologic Engineering Centers – Flood Damage Analysis
HEC-GeoRAS	Hydrologic Engineering Centers – Geospatial River Analysis System
HEC-RAS	Hydrologic Engineering Centers – River Analysis System
LAG	Level at Ground or Grade
LiDAR	Light Detection and Ranging
m	meters
MIN	Minimum
NC	North Carolina
NCFMP	North Carolina Floodplain Mapping Program
NED	National Elevation Dataset
NEEA	National Enhanced Elevation Assessment
NFIP	National Flood Insurance Program
NRC	National Resource Council
O	Observed
Poly	Polygon
RMSE	Root Mean Square Error
SD	Structural Database
SID	Structural Inventory Database
TIN	Triangulated Irregular Network
U.S.	United States
USACE	United States Army Corps of Engineers
USGS	United States Geological Survey
WSP	Water Surface Profile
yr	year

Bibliography

Asheville Field Office (2004). *USGS 03451000 Swannanoa River at Biltmore, NC*. Retrieved from United States Geological Survey (USGS): National Water Information System. http://waterdata.usgs.gov/nwis/rt

Bales, J. D., Oblinger, C. J., & Sallenger, A. H. Jr. (2000). *Two months of flooding in Eastern North Carolina, September - October 1999: Hydrologic water-quality, and geologic effects of Hurricanes Dennis, Floyd, and Irene* (Water-Resources Investigations Report 00-4093). Raleigh, NC: USGS http://pubs.usgs.gov/wri/wri004093/flooding.html

Basgnight, M., Black, J. B., & Easley, M. F. (2005, February 25). *The Hurricane Recovery Act of 2005* (Session 205, Session Law 2005-1, Senate Bill 7).Washington DC: General Assembly of North Carolina

Brown & Caldwell. (2010). *A summary of expected flood damages in the Swannanoa River basin.* Charlotte, NC: Brown and Caldwell Environmental Engineers.

Colby, J. D., & Dobson, J. G. (2010). Flood modeling in the Coastal Plains and Mountains: Analysis of terrain resolution. *Natural Hazards Review*, 11(1), 19-28.

Dawson, W. R. (2003). *Generic depth-damage relationships for residential structures with basements* (Economic guidance memorandum (EGM) 04-01). U.S. Army Corps of Engineers, Chief, Planning and Policy Division, Directorate of Civil Works

Dewberry. (2011). *Final report of the National Enhanced Elevation Assessment.* [Revised March 29, 2012]. Fairfax, VA: Dewberry. Retrieved from http://www.dewberry.com/services/geospatial/national-enhanced-elevation-assessment

Ding, A., White, J. F., Ullman, P. W., & Fashokun, A. O. (2008). Evaluation of HAZUS-MH

flood model with local data and other program. *Natural Hazards Review,* 9(1), 20-28.

European Commission. (2007). Directive 2007/60/EC of the European Parliament and of the

Council: of 23 October 2007: the assessment and management of flood risks. *Official*

Journal of the European Union, L 288, 50.

Federal Emergency Management Agency (FEMA). (2002). *National Flood Insurance*

*Program: Program description.*Washington, DC: FEMA

Federal Emergency Management Agency (FEMA). (2004). Disaster assistance for Tropical

Storm Frances and Hurricane Ivan tops $44 million dollars in North Carolina. Retrieved

from https://www.fema.gov/news-release/2004/11/17/disaster-assistance-tropical-storm-

frances-and-hurricane-ivan-tops-44

Fox, J., Dobson, G., Phillips, M., Pierce, T., & Fox, D. P. (2008). Visualization as a decision

support tool – Asheville's North Fork Resevoir (Buncombe County, North Carolina) and

the balance between drought and flood mitigation. RENCI at UNC-Asheville, Asheville,

NC

Gesch, D. B. (2007). The National Elevation Dataset. In D. F. Maune, J. B. Maitra, & E. J.

McKay, *Digital elevation model technologies and applications: the DEM users manual*

(2nd ed.). American Society for Photogrammetry and Remote Sensing, Bethesda, MD 99-

118.

Gueudet, P., Wells, G., Maidment, D., & Neuenschwander, A. (2004). Influence of the post-spacing of the L1DAR-derived DEM on flood modeling. *Proceedings, 2004 American Water Resources Association Spring Specialty Conference, GIS and Qater Resources III,* Nashville, TN: American Water Resources Association

Hodgson, M. E., Jensen, J., Raber, G., Tullis, J., Davis, B. A., Thompson, G., & Schuckman, K. (2005). An evaluation of LiDAR-derived elevation and terrain slope in leaf-off conditions. *Photogrammetric Engineering & Remote Sensing*, 71(7), 817-823.

Johnson, J. F. (2000). Economic Guidance memorandum (EGM) 01-03, Generic depth-damage relationships. United States Army Corps of Engineers (USACE), Washington, District of Columbia, USA.

Luino, F., Cirio, C. G., Biddoccu, M., Agangi, A., Giulietto, W., Godone, F., & Nigrelli, G. (2009). Application of a model to the evaluation of flood damage. *Geoinformatica*, 13, 339-353.

North Carolina Floodplain Mapping Program (NCFMP). (2006). *LiDAR accuracy assessment report – Buncombe County.* Retrieved from the NC Department of Environment and Natural Resources Division of Energy, Mineral and Land Resources, Floodplain Mapping, Phase III LiDAR Mapping folder http://portal.ncdenr.org/web/lr/geodetic/floodplaininfo

North Carolina Floodplain Mapping Program (NCFMP). (2008). *North Carolina Floodplain Mapping Program: 2000-2008 Program review. Accomplishments, lessons learned, and benefit.* Preliminary Draft October 1, 2008

North Carolina Floodplain Mapping Program (NCFMP). (2014). *Flood risk information system*. Retrieved from http://fris.nc.gov/fris/Home.aspx?ST=NC

National Research Council (NRC). (2007). *Elevation data for floodplain mapping*. Washington, DC: National Academies Press.

National Research Council (NRC). (2009). *Mapping the zone: Improving flood map accuracy.* Washington, DC: National Academies Press.

National Weather Service. (2015). *Swannanoa River at Biltmore.* Greenville-Spartanburg Weather Forecast Office. Retrieved from http://www.water.weather.gov/ahps2/hydrograph.php?wfo=gsp&gage=bltn7

Omer, C. R., Nelson, E. J., & Zundel, A. K. (2003). Impact of varied data resolution on hydraulic modeling and floodplain delineation. *Journal of the American Water Resources Association*, 39(2), 467-475.

Ormond, T. P. (2010). *Swannanoa flood risk management project: replacement cost less depreciation structure values.* Asheville, NC: HydroCycle Engineering, PC

Pine, J. C. (2009). *Environmental Hazards Analysis.* London: Taylor Francis.

Raber, G. T., Jensen, J. R., Hodgson, M. E., Tullis, J. A., Davis, B. A., & Berglund, J. (2007). Impact of LiDAR nominal post-spacing on DEM accuracy and flood zone delineation. *Photogrammetric Engineering & Remote Sensing*, 73(7), 793-804.

Ruiz-Villanueva, V., Bodoque, J. M., Dı́ez-Herrero, A., & Blade, E. (2014). Large wood transport as significant influence on flood risk in a mountain village. *Natural Hazards,* 74, 967-987.

Rulli, M. C., & Rosso, R. (2007). Hydrologic response of upland catchments to wildfires. *Advances in Water Resources*, 30, 2072-2086.

Scawthorn, C., Flores, P., Blais, N., Seligson, H., Tate, E., Chang, S., Mifflin, E., Thomas, W., Murphy, J., Jones, C., & Lawrence, M. (2006). HAZUS-MH flood loss estimation methodology. II: Damage and loss assessment. *Natural Hazards Review*, 7:2(72), 72-81.

Snyder, G. I. (2012). *National enhanced elevation assessment at a glance.* (U.S. Geological Survey Fact sheet 2012-3088). Retrieved from http://pubs.usgs.gov/fs/2012/3088/pdf/fs2012-3088.pdf

Tao, J., & Barros, A. P. (2013). Prospects for flash flood forecasting in mountainous regions - An investigation of Tropical Storm Fay in the Southern Appalachians. *Journal of Hydrology*, 506, 69-89.

Tobler, W. R. (1988). Proc., 1st Meeting of the Int. Geographical Union Global Database Planning Project, H. Mounsey and R.F. Tomlinson eds. *In Building databases for global science: Resolution, resampling and all that.* Taylor and Francis, London, England 129-137.

Turner, A. B., Colby, J. D., Csontos, R. M., & Batten, M. (2013). Flood modeling using a synthesis of multi-platform LiDAR data. *Water*, 5(4), 1533-1560.

URS Group, I. (2006). *Data collection for development of stage damage curves for flooding of commercial properties:* Asheville, NC. Nashville, TN: Department of the Army, Corps of Engineers.

United States Geological Survey (USGS) (2015). *Peak streamflow for North Carolina.* USGS Water Resources, Retrieved from http://nwis.waterdata.usgs.gov/nc/nwis/peak?site_no=03451000&agency_cd=USGS&format=html

Vaze, J., Teng, J., & Spencer, G. (2010). Impact of DEM accuracy and resolution on topographic indices. *Environmental Modeling & Software,* 25, 1086-1098.

Westoby, M. J., Glasser, N. F., Brasington, J., Hambrey, M. J., Quincey, D. J., & Reynolds, J. M. (2014). Modelling outburst floods from moraine-dammed glacial lakes. *Earth-Science Reviews*, 134, 137-159.

Wohl, E. E. (2000). Mountain rivers. American Geophysical Union, *Water Resources Monograph,* 14, 1-320.

Worni, R., Huggel, C., Clague, J. J., Schaub, Y., & Stoffel, M. (2014). Coupling glacial lake impact, dam breach, and flood processes: A modeling perspective. *Geomorphology*, 224, 161-176.

Zhang, W., & Montegomery, D. R. (1994). Digital elevation model grid size, landscape representation, and hydrologic simulations. *Water Resources Research*, 30(4), 1019-1028.

Biographical Information

Monica Davis has obtained four undergraduate degrees and two minors from Purdue University; a Bachelor's of Forestry in Forestry, a Bachelor's of Science in Wildlife Sciences, a Bachelor's of Science in Landscape Horticulture and Design, a Bachelor's of Science in Horticulture Production and Marketing, a Minor in Education, and a Minor in Plant Physiology. Ms. Davis held numerous jobs prior to seeking a Master's degree. Ms. Davis has worked as a Timber Technician for the State of Indiana, as an Assistant Landscape Designer, and as an Office Manager for a large horticulture production company. Ms. Davis began to take graduate level courses in GIS and Remote Sensing at Indiana University Purdue University in preparation for acceptance into a Master's Program.

In August of 2010, Ms. Davis began study towards a Master of Arts degree in Geography at Appalachian State University. After completion of 30 graduate hours of coursework, Ms. Davis obtained two jobs an internship working for Land of Sky Regional Council and a position working as an Environmental GIS Specialist/Forester for Natural Systems Analysts, Inc. Ms. Davis was then offered a full time position as a Geographer for Dewberry in Vienna, Virginia. Upon leaving Dewberry, Ms. Davis chose to complete her thesis requirement for graduation from Appalachian State University in spring of 2015. Ms. Davis looks forward to a long and rewarding career in water resources, GIS, and physical geography with dreams of research and teaching.